

Supporting Information

Mechanistic Investigation of Oxygen Rebound in a Mononuclear Nonheme Iron Complex

Thomas M. Pangia,[†] Vishal Yadav,[†] Emilie F. Gérard,[‡] Yen-Ting Lin,[‡] Sam P. de Visser^{*,‡}, Guy N. L. Jameson[§], and David P. Goldberg^{*,†}

[†]Department of Chemistry, The Johns Hopkins University, 3400 North Charles Street, Baltimore, Maryland, 21218, USA

[‡]Manchester Institute of Biotechnology and School of Chemical Engineering and Analytical Science, The University of Manchester, 131 Princess Street, Manchester M1 7DN, U.K.

[§]School of Chemistry, Bio21 Molecular Science and Biotechnology Institute, The University of Melbourne, 30 Flemington Road, Parkville, Victoria 3052, Australia

Contents

- I. Materials and general methods**
- II. Analytical methods**
- III. Experimental details**
- IV. Supporting figures**
- V. Supporting tables**
- VI. Cartesian coordinates**
- VII. References**

I. Materials and general methods. All chemicals and reagents were purchased from Sigma-Aldrich, Fisher Scientific, Acros Organics, Merck, Fluka Analytical, or Alfa Aesar and were used without further purification unless noted otherwise. Solvents (methanol, diethyl ether, acetonitrile, toluene, and tetrahydrofuran) used in organic synthesis were purified via Pure-Solv Solvent Purification System from Innovative Technology, Inc. Solvents used in the reactions of the iron(II) and iron(III) complexes were subjected to additional purification after initial purification via a Pure-Solv Solvent Purification System. THF and toluene were distilled from sodium/benzophenone and were degassed by freeze-pump-thaw cycles and stored in a N₂ filled dry box. All reactions involving inert atmosphere were performed using standard Schlenk or drybox techniques. The compounds tris(*p*-t-butylphenyl)methyl bromide,¹⁻² tris(*p*-phenylphenyl)methyl bromide,¹ and tris(*p*-cyanophenyl)methyl chloride³ were prepared according to literature procedures. Tris(*p*-methoxyphenyl)methyl chloride was obtained from Alfa-Aesar and used as received. TEMPO radical was obtained from Sigma-Aldrich and used as received. Metal complexes [Fe^{III}(N₃PyO^{2Ph})(OCH₃)](ClO₄) (**1**) and ⁵⁷**1** were prepared as previously described.⁴ *Caution: Perchlorate salts of metal complexes are potentially explosive. Although this lab did not encounter any incidents, care should be taken when handling these compounds. Note: The trityl radical derivatives are O₂ and light-sensitive. Measures should be taken to avoid exposure of the radical to light and air.*

II. Analytical methods. Kinetic UV-vis measurements were performed on a Hewlett-Packard Agilent 8453 diode-array spectrophotometer with a 3.5 mL quartz cuvette (path length = 1 cm) equipped with a septum. Other UV-visible spectra were recorded on a Varian Cary 50 Bio spectrophotometer, or a Varian Cary 60 Bio spectrophotometer. NMR spectra were collected on a Bruker Avance 400 MHz FT-NMR spectrometer. Mössbauer spectra were recorded on a spectrometer from SEE Co. (Edina, MN) operating in the constant acceleration mode in a transmission geometry. The sample was kept in an SVT-400 cryostat from Janis Research Co. (Wilmington, MA), and liquid N₂ was used as a cryogen for 80 K measurements. Isomer shifts were determined relative to the centroid of the spectrum of a metallic foil of α -Fe collected at room temperature. Data analysis was performed using version F of the program WMOSS (www.wmoss.org), and quadrupole doublets were fit to Lorentzian lineshapes. Mössbauer samples

were prepared in custom-made Delrin cups and frozen in liquid nitrogen prior to use. Data collection were performed in constant acceleration mode in zero magnetic field.

III. Experimental Details.

Synthesis of derivatives of trityl radical ($4\text{-X-C}_6\text{H}_4)_3\text{C}\cdot$ (X = OMe, tBu, Ph, CN). These derivatives were generated *in situ* in toluene as monomers in solution from copper or zinc according to previously published procedure.^{1,3} Difficulties in producing high yields of each radical at concentrations >10 mM limited the range of concentrations that could be employed for the reactions with **1**.

Reaction of **1 with ($4\text{-tBu-C}_6\text{H}_4)_3\text{C}\cdot$. UV-vis Spectroscopy.** A solution of **1** (3 mL, 0.6 mM) in THF was placed in a quartz cuvette (1 cm pathlength). An amount of ($4\text{-tBu-C}_6\text{H}_4)_3\text{C}\cdot$ (5 equiv) was prepared in situ in toluene and added directly to the solution of **1** in the quartz cuvette via gas-tight syringe. To observe the reactivity of **1** and ($4\text{-tBu-C}_6\text{H}_4)_3\text{C}\cdot$, the UV-vis band at $\lambda_{\max} = 570$ nm (**1** in THF) was monitored over 5 min. Decay (~80%) of the peak at 570 nm was observed over the time period, marking the consumption of complex **1** (Figure S1).

Generation of ($4\text{-CN-C}_6\text{H}_4)_3\text{C}\cdot$ and measurement of extinction coefficient. The compound was prepared according to a previous literature procedure.³ To an amount of tris(*p*-cyanophenyl)methyl chloride (9.61 mM) was added excess zinc powder (Zn), and then toluene (5.5 mL) was added and the mixture and was stirred in the dark for 90 min at 75 °C. The pink solution was cooled to 23 °C, filtered through Celite®, then immediately used for kinetics experiments. UV-vis (toluene): λ_{\max} (ϵ , M⁻¹ cm⁻¹): 568 (290). Radical yield (EPR) = 6.3 mM, 65%. The yield was obtained from quantification of the radical concentration by EPR spectroscopy at 23 °C (parameters: frequency = 9.75 GHz, power = 0.2 mW, receiver gain = 5.02 x 10³, mod freq = 100 kHz, mod amp = 0.1 G). The EPR signal was quantified through double integration and comparison with a TEMPO radical standard calibration curve under nonsaturating conditions. The measurement was performed in duplicate. Beer's Law ($\epsilon = A/bc$) was used to calculate the extinction coefficient, where A is absorbance of the stock solution at the maximum wavelength, b is the path length of

the UV-vis cuvette (1 cm), and c is the radical concentration in M determined from EPR spectroscopy.

Kinetic study of reactions between **1 and trityl radical derivatives.** Under light-limiting conditions, trityl derivatives $(4\text{-X-C}_6\text{H}_4)_3\text{C}\cdot$ ($\text{X} = \text{OMe}$, $t\text{Bu}$, Ph, CN) were freshly prepared in toluene according to literature procedures.¹ The concentrations of each radical was determined by measuring the UV-vis spectrum and using the extinction coefficients for each radical derivative. $(4\text{-X-C}_6\text{H}_4)_3\text{C}\cdot$ ($\text{X} = \text{OMe}$, $\epsilon = 570 \text{ M}^{-1} \text{ cm}^{-1}$; $\text{X} = t\text{Bu}$, $\epsilon = 750 \text{ M}^{-1} \text{ cm}^{-1}$; $\text{X} = \text{Ph}$, $\epsilon = 580 \text{ M}^{-1} \text{ cm}^{-1}$; $\text{X} = \text{CN}$, $\epsilon = 290 \text{ M}^{-1} \text{ cm}^{-1}$). Varying amounts of stock solution for each radical were prepared (200 – 1000 μL) and diluted to 2 mL in toluene. An amount of **1** in THF was added (100 μL , 4 mM) to a solution of radical in toluene to begin the reaction. Spectral changes showed consumption of **1** (Figures S2-S5). Pseudo-first-order rate constants (k_{obs}) for these reactions were obtained using the software Kaleidograph 4.5 through nonlinear least-squares fitting of plots of absorbance at 570 ($\text{X} = \text{OMe}$, $t\text{Bu}$) or 590 ($\text{X} = \text{CN}$) or 680 ($\text{X} = \text{Ph}$) nm (Abs_t) versus time (t) according to the equation $\text{Abs}_t = \text{Abs}_f - (\text{Abs}_f - \text{Abs}_0) * \exp(-k_{\text{obs}} * t)$, where Abs_0 is the initial absorbance and Abs_f is the final absorbance. Data were fit beginning at 5 s after initial mixing to ensure a homogeneous reaction mixture at the beginning of the kinetics measurements. All plots were extended out to 4 half-lives. Independent measurement of the Fe^{II} complex in the same solvent mixture (toluene/THF 20/1) shows a broad peak at 590 nm ($\epsilon = \sim 650 \text{ M}^{-1} \text{ cm}^{-1}$), which likely accounts for the residual absorbance observed at the end of the radical reactions. There is a separate, slower decay phase of the final absorbance after ~ 4 half-lives which cannot be definitively assigned, but may arise from further decay of the iron(II) product. Second-order rate constants were found from the best-fit line from the plot of k_{obs} versus concentration of radical.

Reaction of **1 with $(4\text{-}t\text{Bu-C}_6\text{H}_4)_3\text{C}\cdot$. ¹H NMR Spectroscopy.** A solution of **1** (0.7 mL, 3 mM) in THF- d_8 was made and an initial spectrum was recorded. Freshly prepared $(4\text{-}t\text{Bu-C}_6\text{H}_4)_3\text{C}\cdot$ (5 equiv) was added and a subsequent spectrum was recorded after 5 min. Formation of a peak at δ 3.00 indicated production of $(4\text{-}t\text{Bu-C}_6\text{H}_4)_3\text{COCH}_3$. A yield of 71% for $(4\text{-}t\text{Bu-C}_6\text{H}_4)_3\text{COCH}_3$ (based on **1**) was observed by integration and comparison with an internal standard ($4\text{-Ph-C}_6\text{H}_4\text{-OCH}_3$) (Figure S8).

Reaction of 1 with (4-tBu-C₆H₄)₃C•. Mössbauer Spectroscopy. A freshly prepared solution of (4-tBu-C₆H₄)₃C• was generated in toluene (0.4 mL) and was added to a solution of ⁵⁷1 in THF at 23 °C (0.8 mL). The final concentration of ⁵⁷1 was 4 mM and (4-tBu-C₆H₄)₃C• was 6 mM. A portion of the reaction mixture (0.5 mL) was added to a Delrin sample holder and the resulting solution frozen in liquid N₂ after 15 min reaction time (Figure S10). An additional aliquot (0.5 mL) from the same reaction mixture was combined with acetonitrile (0.1 mL), added to a Delrin sample holder and the resulting solution frozen in liquid N₂. Mössbauer spectra were measured at 80 K.

Reaction of 1 with Ph₃C⁺. UV-vis Spectroscopy. A solution of 1 (2 mL, 0.5 mM) in THF was placed into a quartz cuvette (1 cm pathlength) and an initial spectrum recorded at 23 °C. An amount of Ph₃(BF₄) (4 equiv in 0.1 mL THF) was added. The UV-vis band at $\lambda_{\text{max}} = 570 \text{ nm}$ (**1** in THF) was consumed within 2 seconds, and a new band at $\lambda_{\text{max}} = 610 \text{ nm}$ was observed (Figure S7).

Reaction of 1 with Ph₃C⁺. ¹H NMR Spectroscopy. The ¹H NMR spectrum of **1** (0.7 mL, 5.0 mM) in THF-*d*₈ was recorded at 23 °C. An amount of Ph₃C(BF₄) (4 equiv) was added and the solution manually mixed in the NMR tube. A spectrum of the reaction mixture was recorded after 5 min at 23 °C, and showed formation of a peak at 3.04 ppm matching the –OCH₃ signal of Ph₃COCH₃. Integration of this peak against an internal standard (Ph-C₆H₄-OCH₃) gave a yield of 80% for Ph₃COCH₃ (based on **1**, Figure S9).

Reaction of 1 with Ph₃C⁺. Mössbauer Spectroscopy.

A solution of ⁵⁷1 (0.4 mL) in THF was combined with Ph₃C(BF₄) in THF (0.2 mL, 4 equiv) at 23 °C. The final concentration of ⁵⁷1 was 4 mM and Ph₃C(BF₄) was 16 mM. An aliquot (0.5 mL) was added to a Delrin sample holder and frozen in liquid N₂ after 5 min of reaction time (Figure S10). Mössbauer spectra were measured at 80 K (Figure S10).

Computational Methods. All calculations were conducted using Gaussian-09⁵ at the UB3LYP level of theory.⁶⁻⁷ Geometry optimizations, frequencies and constraint geometry scans were performed at UB3LYP with the LANL2DZ basis set on iron with core potential and 6-31G* basis set on all other atoms: basis set BS1.⁸⁻⁹ Single point calculations using the LACV3P+ basis set on

iron and 6-311+G* on all other atoms (basis set BS2) were carried out in order to refine the quality of the energies. Further single point calculations at B3LYP/BS2 were done including the continuum polarized conductor model (CPCM) with a dielectric constant mimicking acetonitrile.¹⁰ Free energies reported include solvent, entropic (at 298 K) and zero-point corrections. Transition states were characterized by a single imaginary frequency for the correct mode (C–O stretch vibration), while all local minima had real frequencies only. Calculations were mostly focused on quintet spin reactant pathways, i.e. started from $^6[\text{Fe}(\text{OH})(\text{N3PyO}^{2\text{Ph}})]^+$ and $^6[\text{Fe}(\text{OCH}_3)(\text{N3PyO}^{2\text{Ph}})]^+$, and their reactivities with doublet spin $^2(4\text{-Cl-C}_6\text{H}_4)_3\text{C}^\bullet$ substrates. The reactant complexes (**R_{Cl}**), C–O bond formation transition states (**T_{ScI}**) and alcohol product complexes (**P_{rCl}**) were calculated in the overall quintet and septet spin states. In general, the septet spin transition states and product complexes were substantially higher in energy than the quintet spin states. Previously, we tested a range of density functional methods for calculating oxygen atom transfer reactions by nonheme iron(IV)-oxo to thioanisole.¹⁵ These studies identified UB3LYP with solvent model as a highly suitable method for reproducing experimental enthalpies of activation of oxygen atom transfer reactions; hence this method was applied here.

IV. Supporting figures.

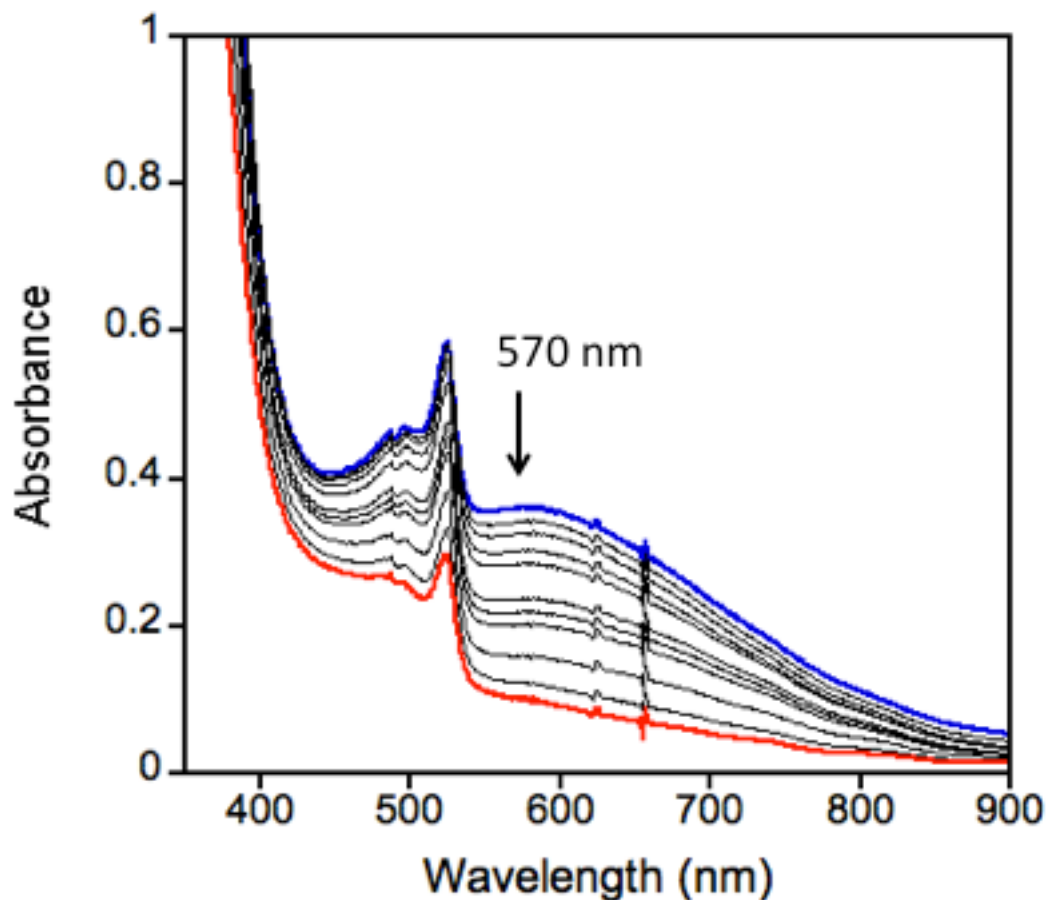


Figure S1. Reaction of **1** and $(4\text{-tBu-C}_6\text{H}_4)_3\text{C}\cdot$ in THF/toluene at 23 °C monitored by UV-vis spectroscopy. Spectra were recorded from 0 – 5 min. Initial spectrum (dark blue line) at 0 min, final spectrum (red line) at 5 min.

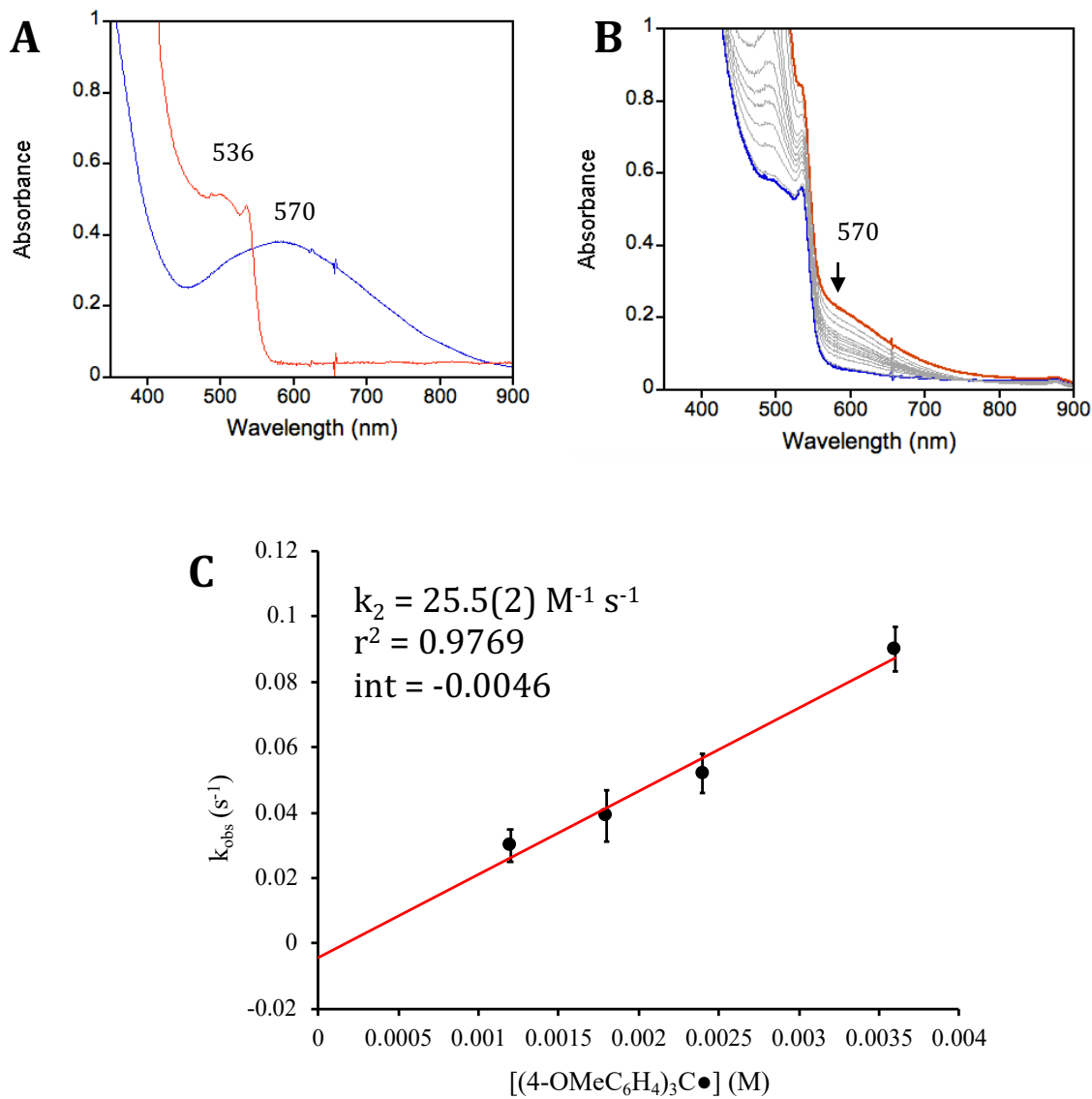


Figure S2. a) Overlay of UV-vis spectra for **1** (blue) and $(4\text{-OMe-C}_6\text{H}_4)_3\text{C}\bullet$ (red). b) Time-resolved UV-vis spectral change for the reaction between **1** (200 μM) and $(4\text{-OMe-C}_6\text{H}_4)_3\text{C}\bullet$ (2.43 mM) at 23 $^\circ\text{C}$. c) Second-order plot of k_{obs} (s^{-1}) vs $[(4\text{-OMe-C}_6\text{H}_4)_3\text{C}\bullet]$ (M) (black circles and red best-fit line).

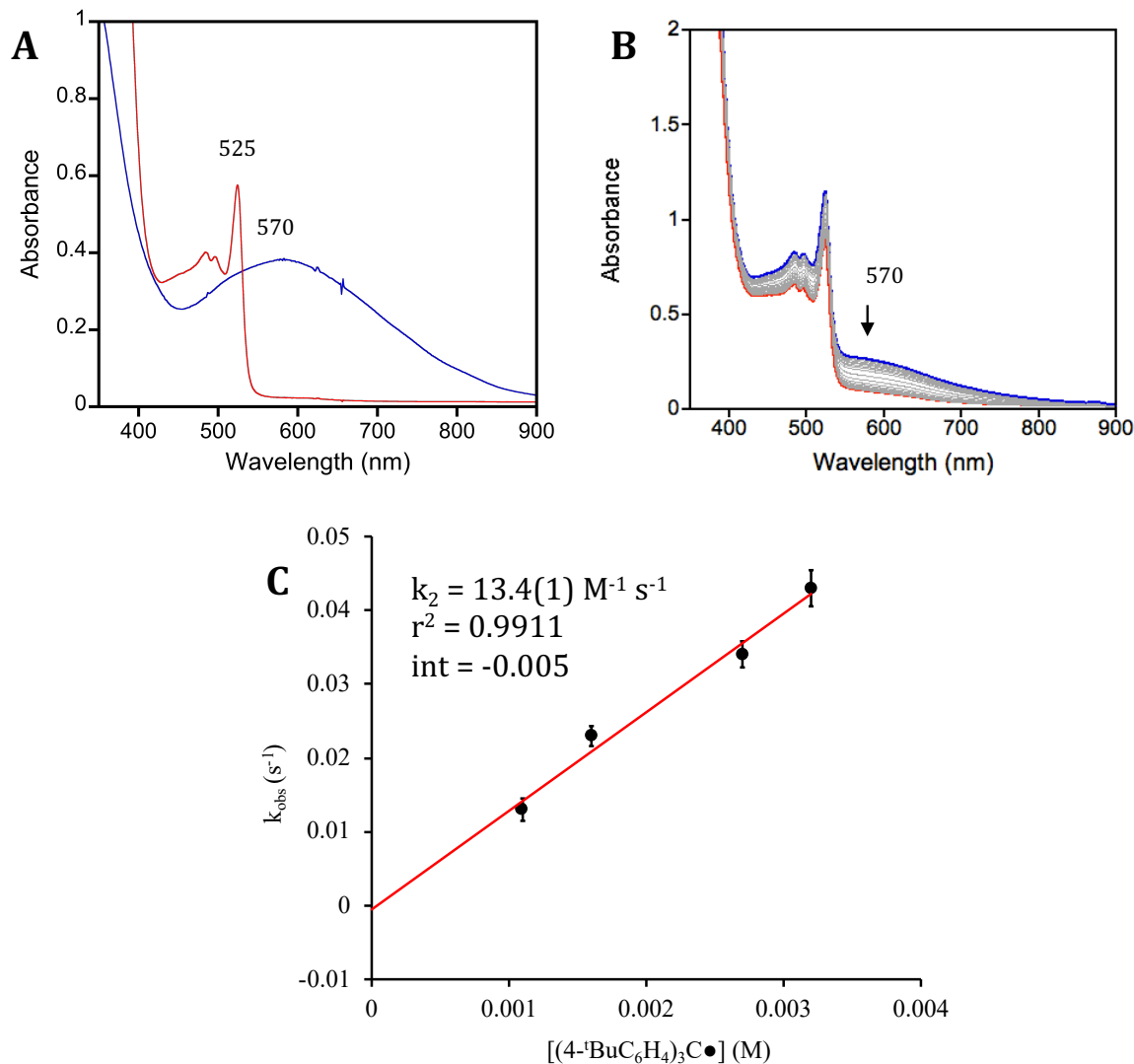


Figure S3. a) Overlay of UV-vis spectra for **1** (blue) and $(4\text{-tBu-C}_6\text{H}_4)_3\text{C}\bullet$ (red). b) Time-resolved UV-vis spectral change for the reaction between **1** (200 μM) and $(4\text{-tBu-C}_6\text{H}_4)_3\text{C}\bullet$ (1.24 mM) at 23 °C. c) Second-order plot of k_{obs} (s^{-1}) vs $[(4\text{-tBu-C}_6\text{H}_4)_3\text{C}\bullet]$ (M) (black circles and red best-fit line).

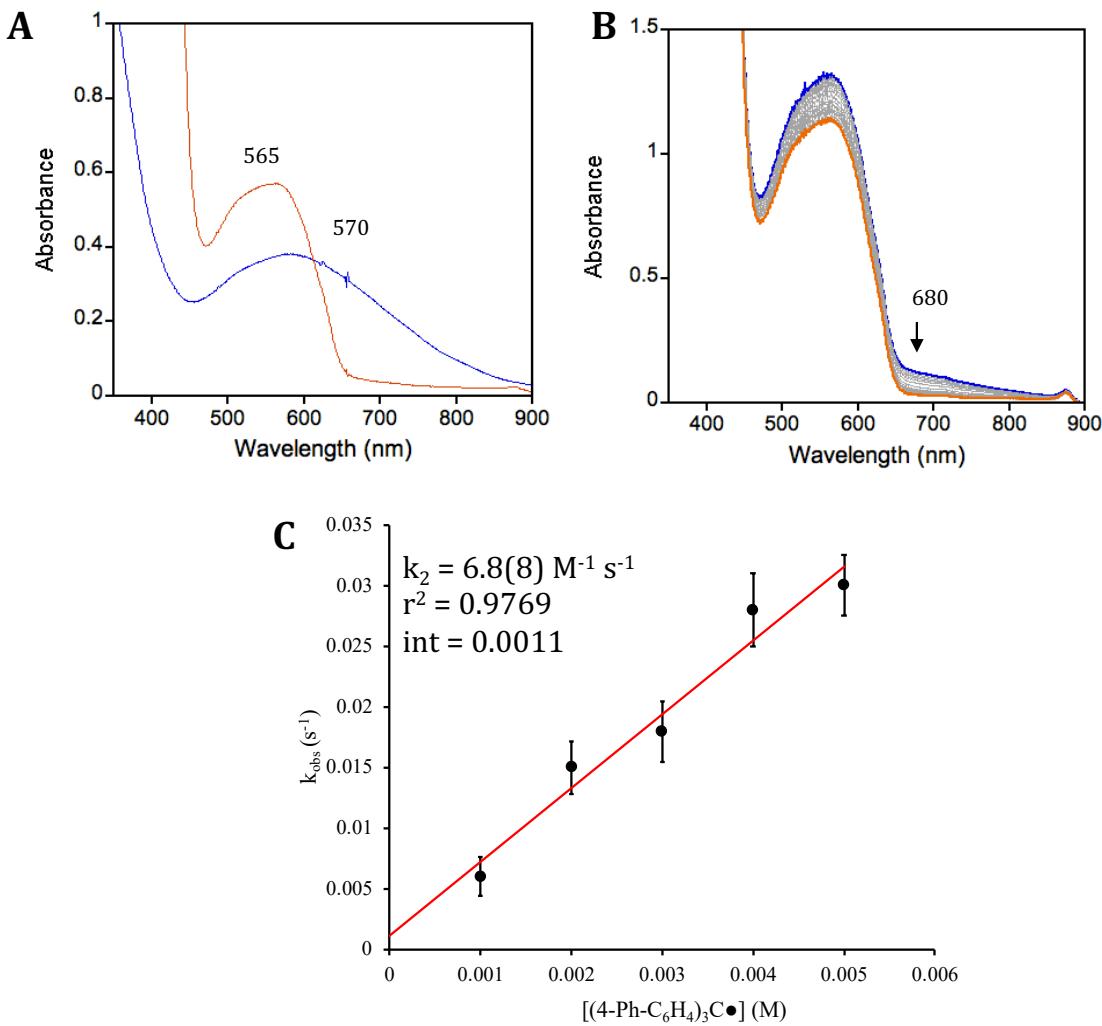


Figure S4. a) Overlay of UV-vis spectra for **1** (blue) and $(4\text{-Ph-C}_6\text{H}_4)_3\text{C}\cdot$ (orange). b) Time-resolved UV-vis spectral change for the reaction between **1** ($200 \mu\text{M}$) and $(4\text{-Ph-C}_6\text{H}_4)_3\text{C}\cdot$ (2.02 mM) at 23°C . c) Second-order plot of k_{obs} (s^{-1}) vs $[(4\text{-Ph-C}_6\text{H}_4)_3\text{C}\cdot]$ (M) (black circles and red best-fit line).

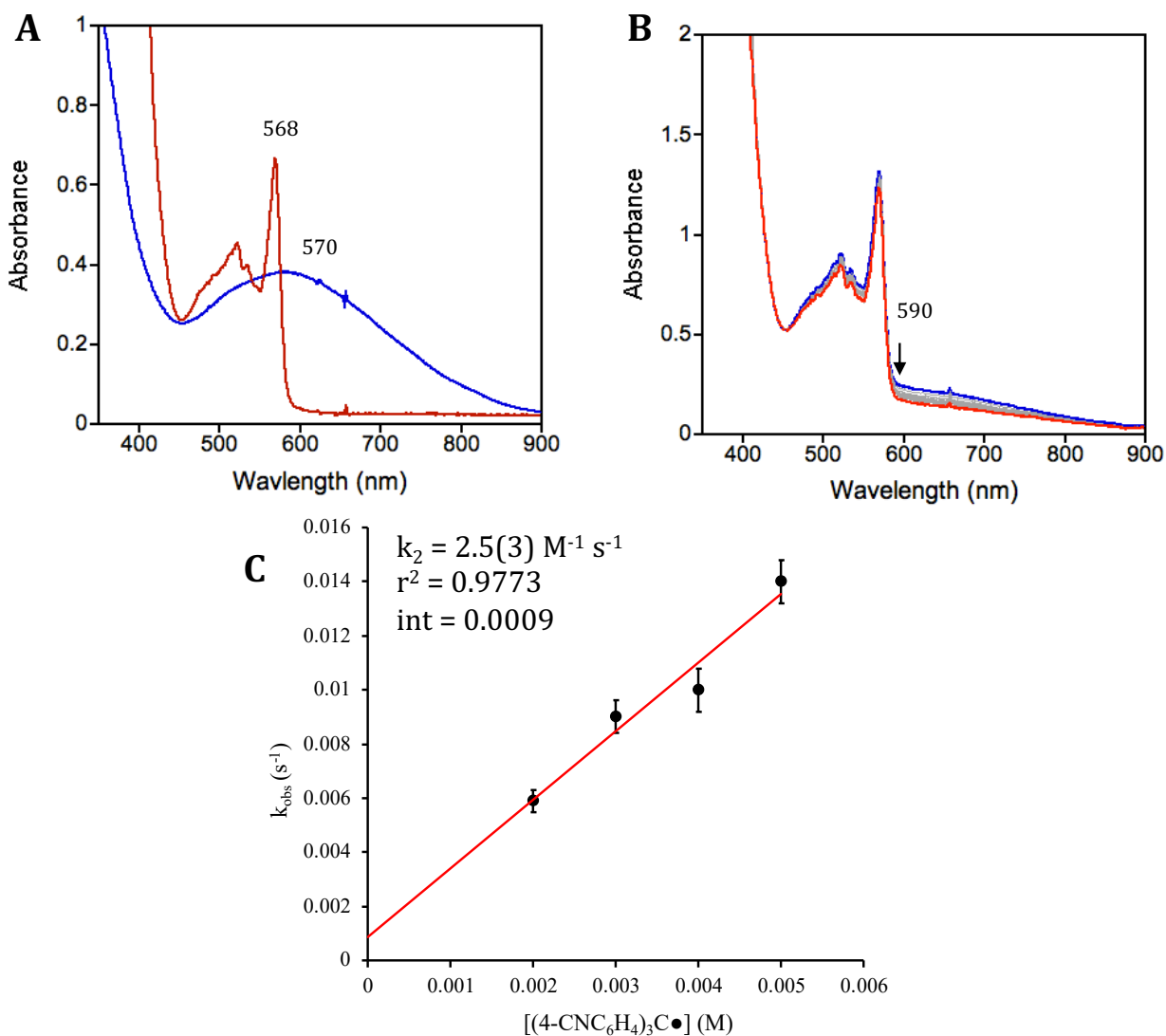


Figure S5. a) Overlay of UV-vis spectra for **1** (blue) and $(4\text{-CN-C}_6\text{H}_4)_3\text{C}\cdot$ (orange). b) Time-resolved UV-vis spectral change for the reaction between **1** ($200 \mu\text{M}$) and $(4\text{-CN-C}_6\text{H}_4)_3\text{C}\cdot$ (4.0 mM) at 23°C . c) Second-order plot of k_{obs} (s^{-1}) vs $[(4\text{-CN-C}_6\text{H}_4)_3\text{C}\cdot]$ (M) (black circles and red best-fit line).

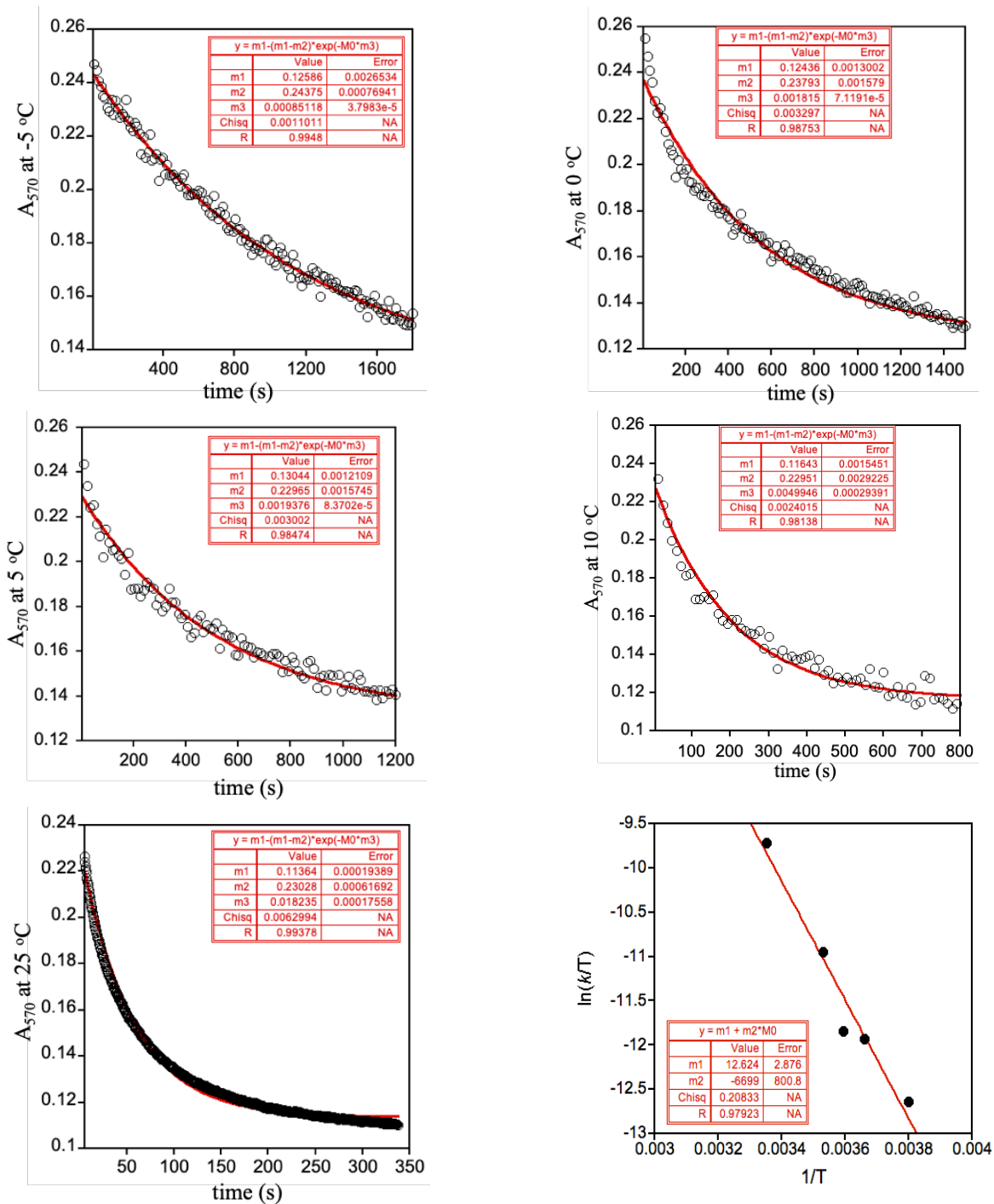


Figure S6. Plots of A_{570} versus time for reactions of **1** (0.2 mM) with $(p\text{-tBu-C}_6\text{H}_4)_3\text{C}\cdot$ (10 equiv) at different temperatures (-10 °C to 25 °C) and Eyring plot ($\ln(k/T)$ versus $1/T$) (black circles = experimental data, red line = best fit).

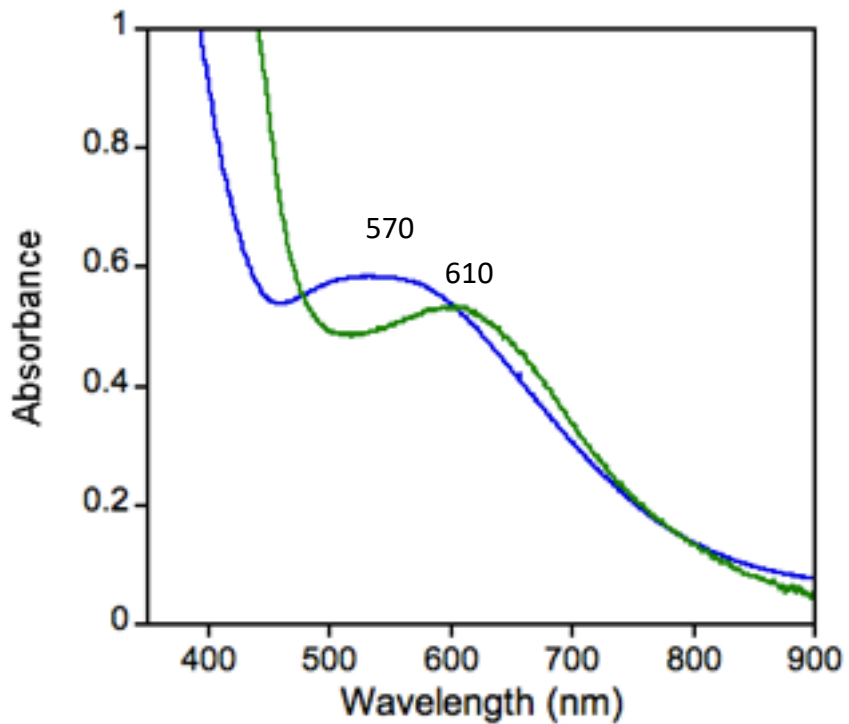


Figure S7. Reaction of **1** and $\text{Ph}_3\text{C}(\text{BF}_4)$ in THF at 23 °C, monitored by UV-vis spectroscopy. **1** (570 nm) is rapidly consumed. Initial spectrum (blue): **1**; final spectrum (green): after 1 min.

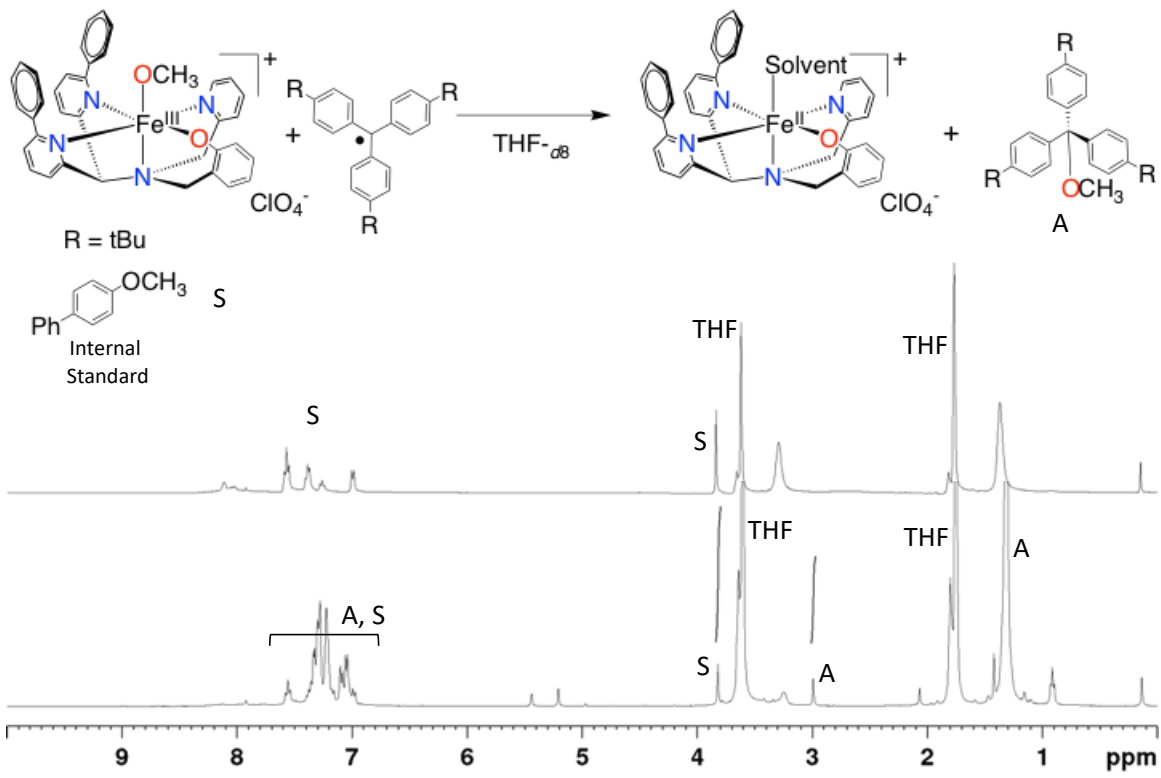


Figure S8: Reaction of **1** and $(4-\text{tBu-C}_6\text{H}_4)_3\text{C}\cdot$ monitored by ^1H NMR in THF-d_8 at 23°C . Top: **1** and internal standard (S) before addition of $(4-\text{tBu-C}_6\text{H}_4)_3\text{C}\cdot$. Bottom: **1** and $(4-\text{tBu-C}_6\text{H}_4)_3\text{C}\cdot$ after 5 min. The $-\text{OCH}_3$ peak of $(4-\text{tBu-C}_6\text{H}_4)_3\text{COCH}_3$ at 3.00 ppm was integrated against the internal standard $-\text{OCH}_3$ peak at 3.83 ppm. Only the diamagnetic region of the spectrum is shown to highlight the organic products.

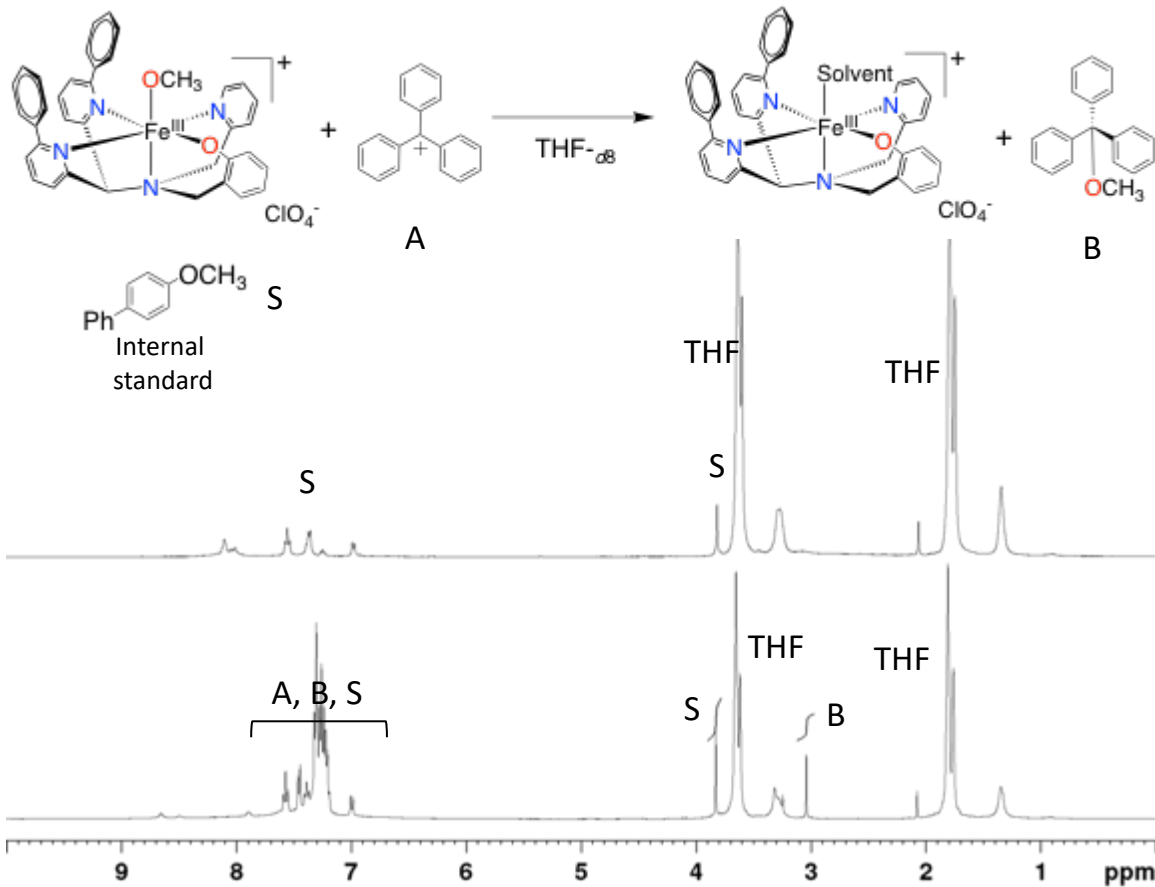


Figure S9. Reaction of **1** and Ph_3C^+ in $\text{THF}-d_8$ for 5 min at 23 °C as monitored by ^1H NMR spectroscopy. Top: **1** and $4\text{-Ph-C}_6\text{H}_4\text{-OCH}_3$ (internal standard **S**) before addition of Ph_3C^+ . Bottom: **1** and Ph_3C^+ after 5 min. Following the reaction, the -OCH_3 peak of the product Ph_3COCH_3 at 3.04 ppm was integrated against the internal standard ($4\text{-Ph-C}_6\text{H}_4\text{-OCH}_3$) – -OCH_3 peak at 3.83 ppm.

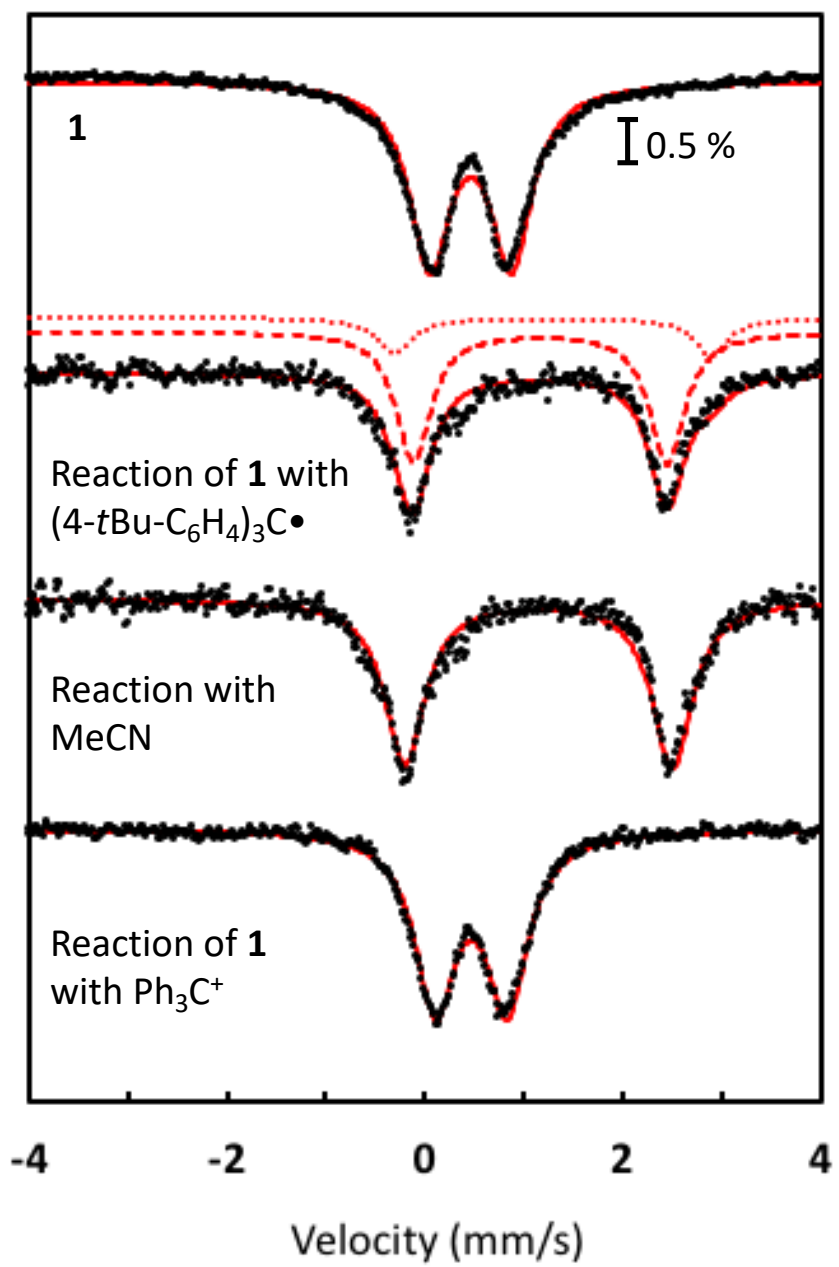


Figure S10. Top: ^{57}Fe Mössbauer spectrum for **1** (dotted line) in THF showing the experimental data (dotted line) and best fit (red line) for a fast-relaxing quadrupole doublet as the major component; top middle: spectrum of the reaction mixture of **1** with $(4\text{-}t\text{Bu-C}_6\text{H}_4)_3\text{C}\bullet$ in a ~2:1 mixture of THF:toluene reacted at 23 °C for 15 min (dotted line) and fitted with two Fe^{II} quadrupole doublets (red dotted and dashed) in a ratio of 4:1; bottom middle: spectrum of the reaction mixture of **1** with $(4\text{-}t\text{Bu-C}_6\text{H}_4)_3\text{C}\bullet$ in a mixture of THF:toluene with addition of acetonitrile (dotted line), and the best fit for a Fe^{II} quadrupole doublet (red line). Bottom: spectrum of the reaction mixture of **1** with Ph_3C^+ (dotted line) with the best fit for a Fe^{III} quadrupole doublet (red line).

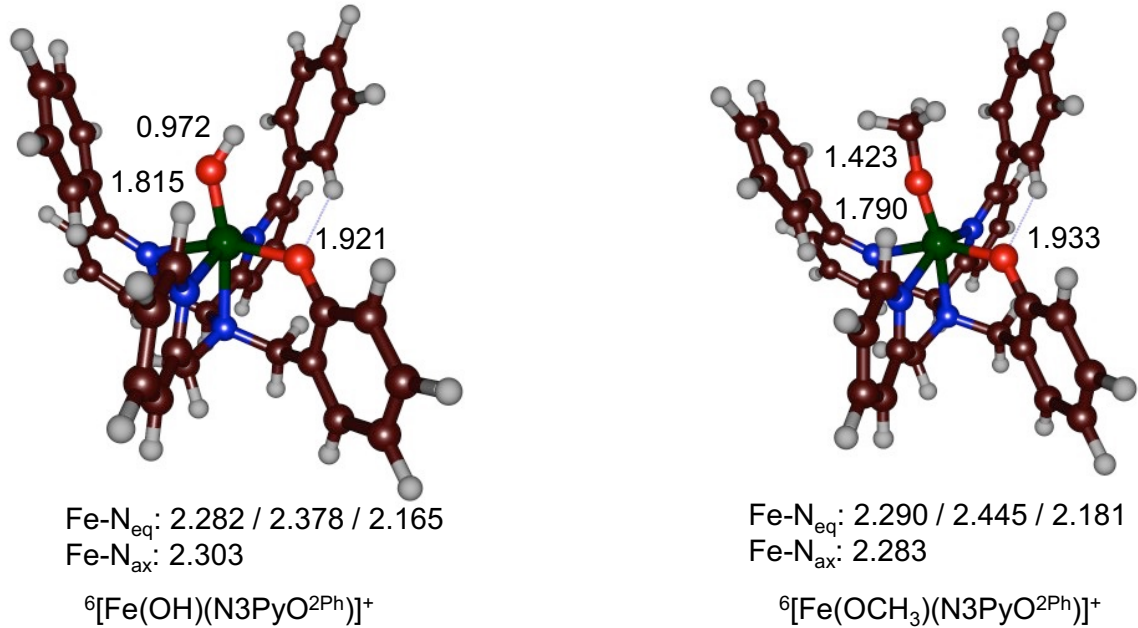


Figure S11. Optimized geometries of ${}^6[\text{Fe}(\text{OH})(\text{N3PyO}^{2\text{Ph}})]^+$ and ${}^6[\text{Fe}(\text{OCH}_3)(\text{N3PyO}^{2\text{Ph}})]^+$ as obtained at UB3LYP/BS1 in Gaussian-09. Bond lengths are in angstroms.

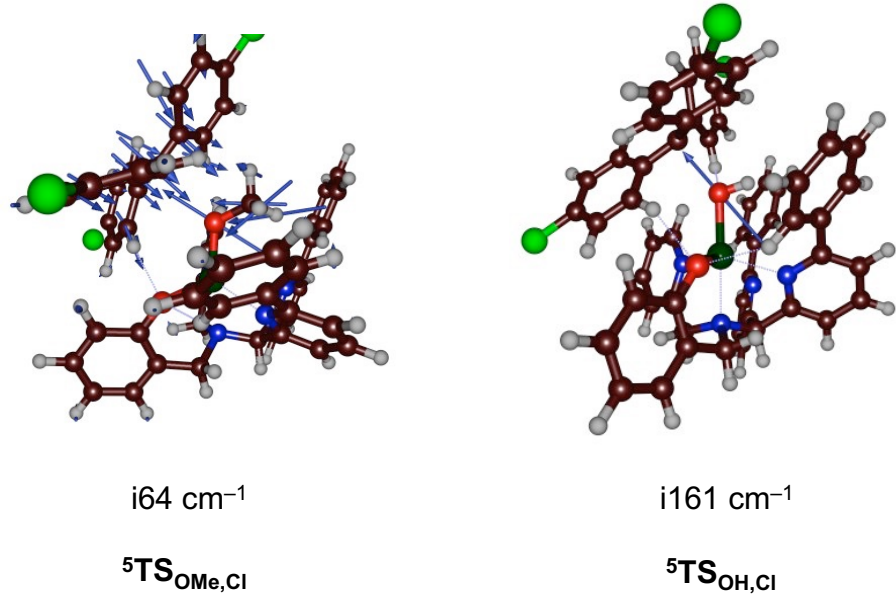


Figure S12. Transition state vectors (in blue) of the imaginary frequencies of ${}^5\text{TS}_{\text{OMe},\text{Cl}}$ and ${}^5\text{TS}_{\text{OH},\text{Cl}}$. As can be seen, both represent C-O bond stretches, although more movement in substrate and methyl groups is visible in the OMe transfer reaction.

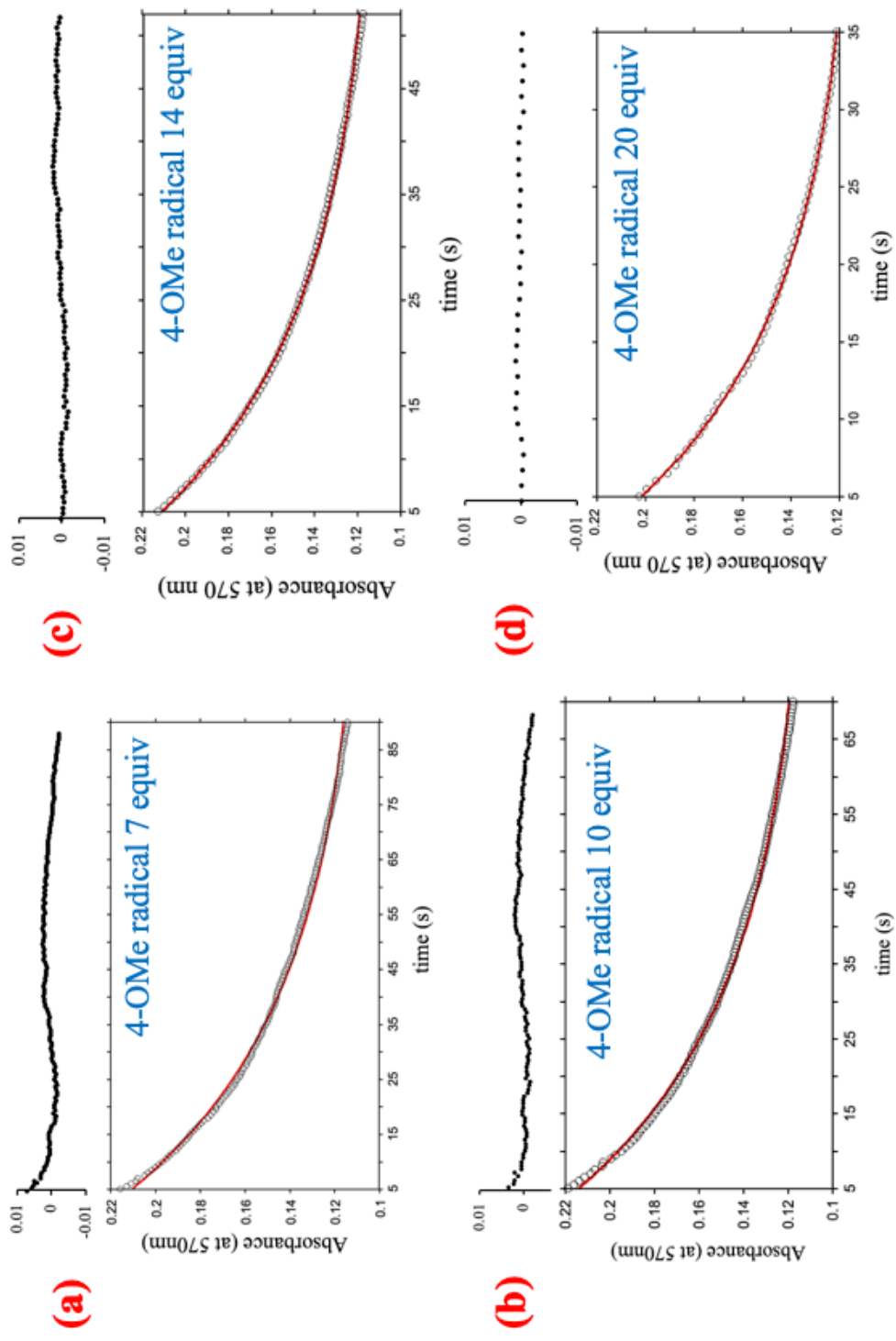


Figure S13. Change in absorbance vs time for the consumption of **1** (black circles) and best-fit (red line) with different equivalents of $(4\text{-OMe-C}_6\text{H}_4)_3\text{C}\cdot$ radical. Residuals are shown at the top of each plot.

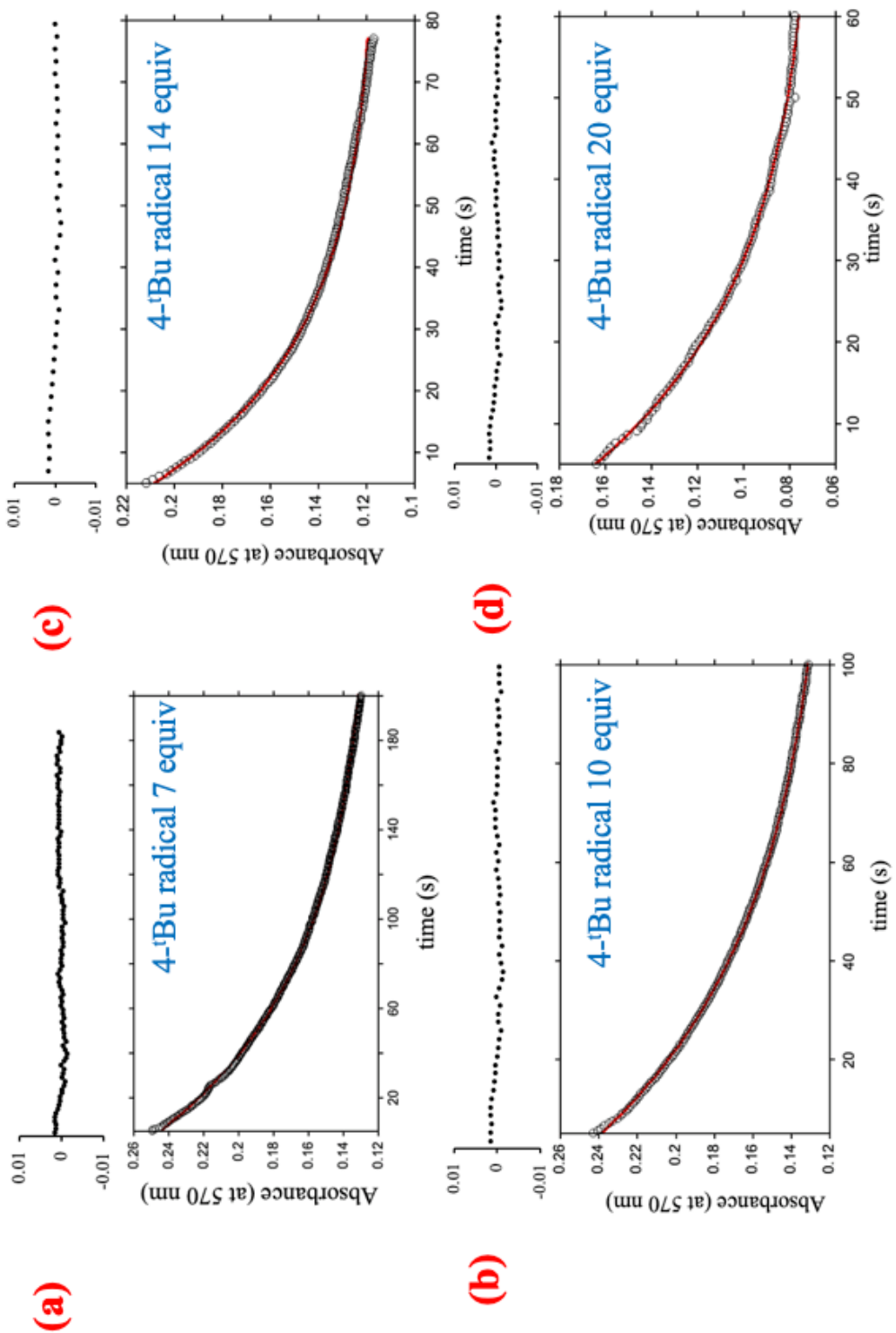


Figure S14. Change in absorbance vs time for the consumption of **1** (black circles) and best-fit (red line) with different equivalents of $(4\text{-}^t\text{Bu-C}_6\text{H}_4)_3\text{C}\cdot$ radical. Residuals are shown at the top of each plot.

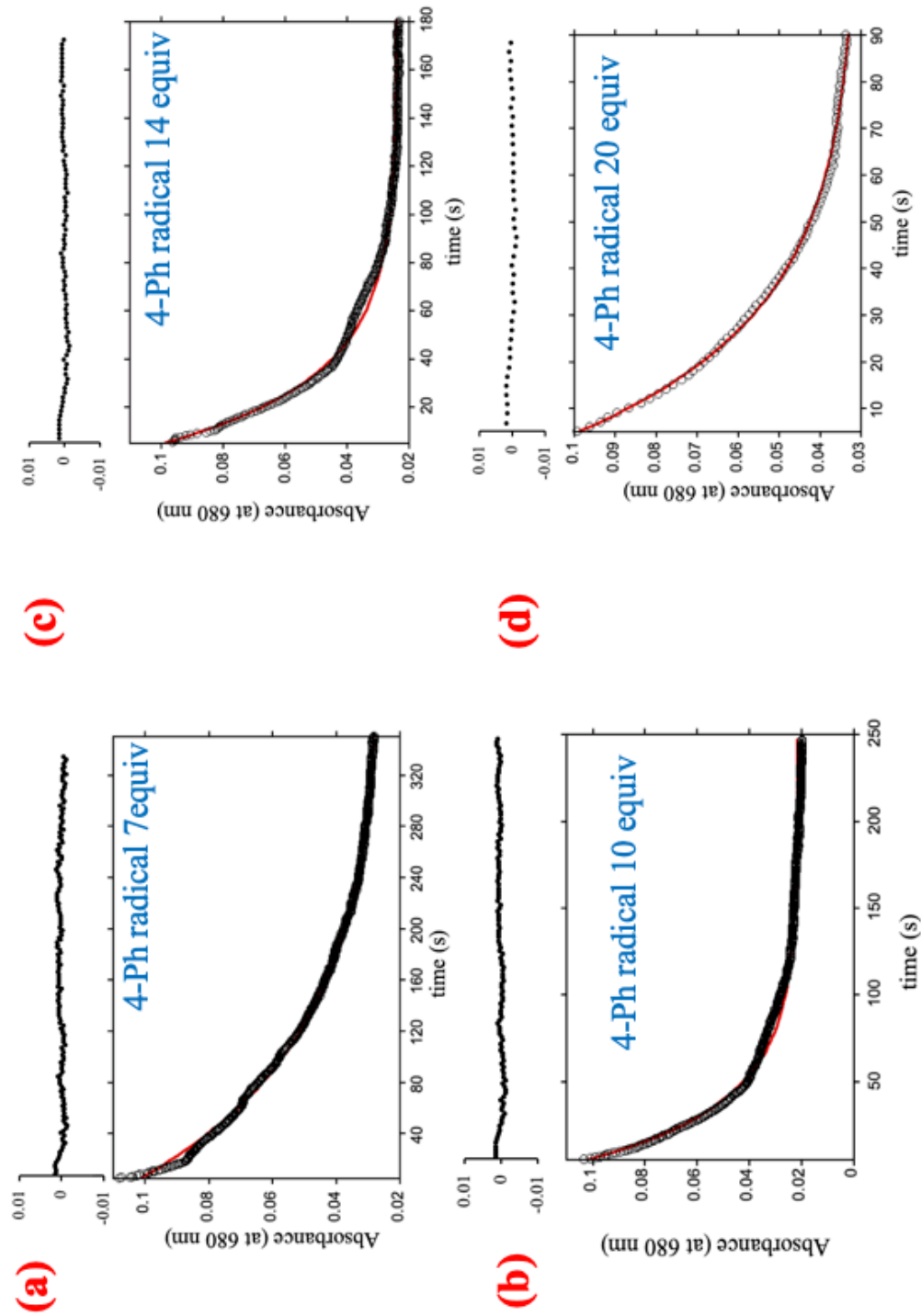


Figure S15. Change in absorbance vs time for the consumption of **1** (black circles) and best-fit (red line) with different equivalents of $(4\text{-Ph-C}_6\text{H}_4)_3\text{C}^\bullet$ radical. Residuals are shown at the top of each plot.

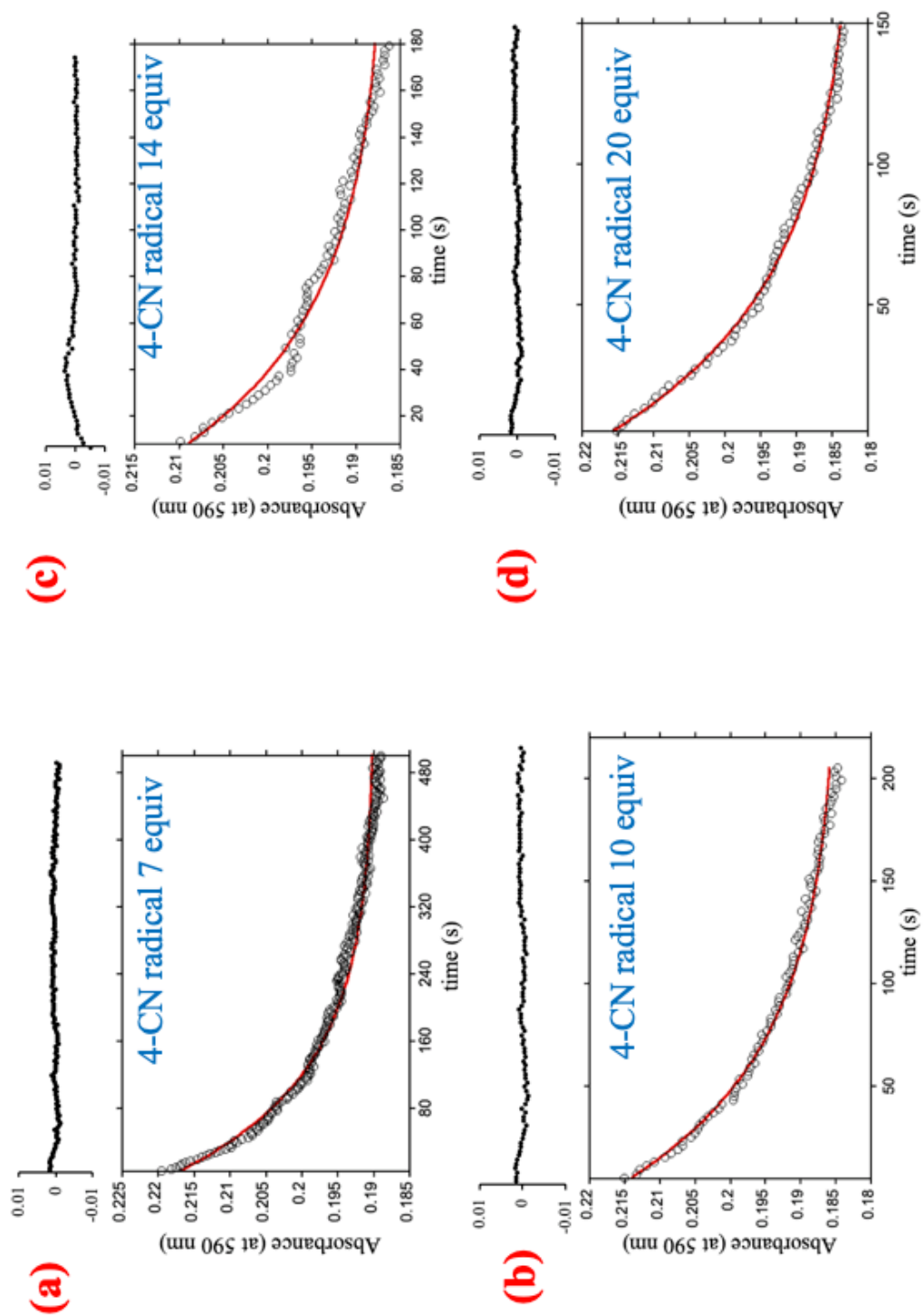


Figure S16. Change in absorbance vs time for the consumption of **1** (black circles) and best-fit (red line) with different equivalents of $(4\text{-CN-C}_6\text{H}_4)_3\text{C}^\bullet$ radical. Residuals are shown at the top of each plot.

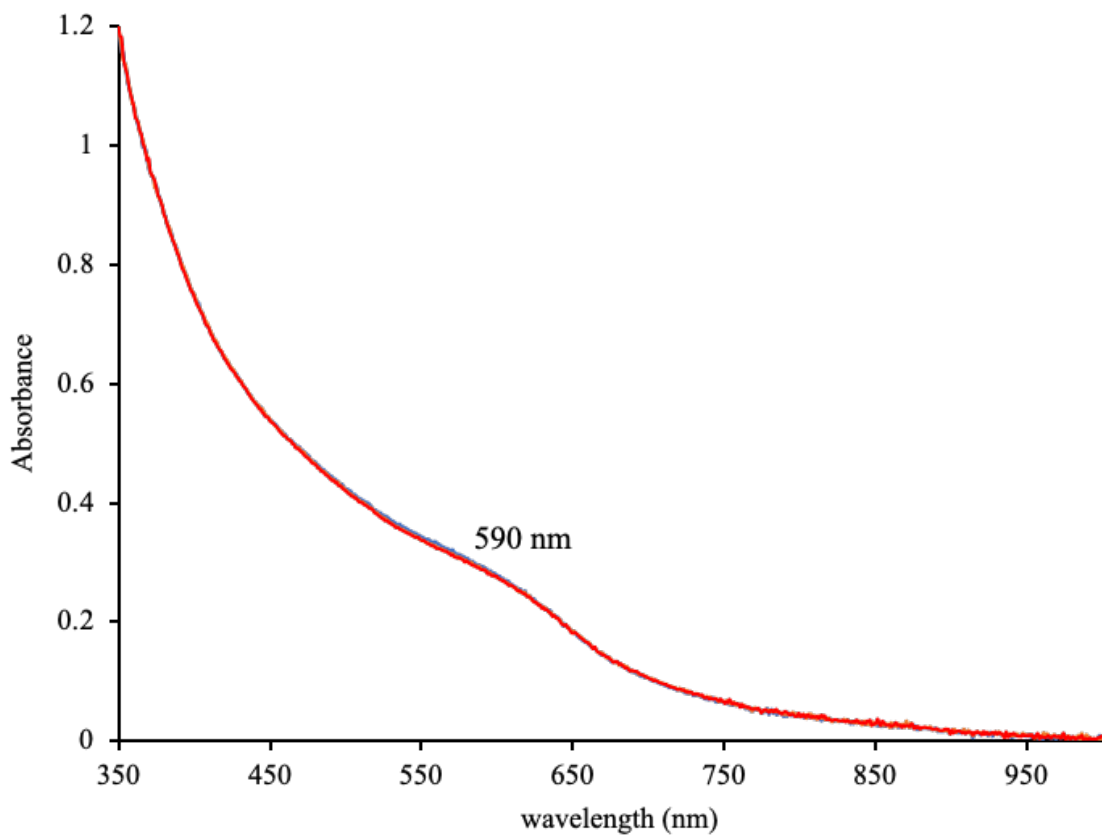


Figure S17. UV-vis spectrum of Fe(II) complex (400 μ M) in toluene-THF (20/1).

V. Supporting tables.

Table S1. ^{57}Fe Mössbauer parameters for **1**, reaction of **1** with 4-(tBu-C₆H₄)₃C•, and reaction of **1** with Ph₃C⁺.

	T (K)	Species	δ (mm/s)	ΔE_Q (mm/s)	$\Gamma_{L(R)}$ (mm/s)	I (%)
1	80	hs-Fe ^{III}	0.48	0.87	0.83 (0.83)	90
1 and 4-(tBu-C ₆ H ₄) ₃ C•	80	hs-Fe ^{II}	1.29	3.19	0.44 (0.44)	20
		hs-Fe ^{II}	1.16	2.56	0.42 (0.42)	80
1 and 4-(tBu-C ₆ H ₄) ₃ C•, MeCN	80	hs-Fe ^{II}	1.16	2.66	0.49 (0.49)	90
1 and Ph ₃ C ⁺	80	hs-Fe ^{III}	0.45	0.72	0.82 (0.82)	90

Table S2. Group spin densities of UB3LYP/BS1 optimized geometries for the reaction pathway from $\text{Re}_{\text{Cl},\text{OH}}$ as obtained in Gaussian-09.

	ρ_{Fe}	ρ_{ligand}	ρ_{OH}	ρ_{SubCl}
${}^5\text{Re}_{\text{Cl},\text{OH}}$	3.98	0.65	0.37	-1.00
${}^5\text{TS}_{\text{Cl},\text{OH}}$	3.81	0.31	0.20	-0.32
${}^5\text{Pr}_{\text{Cl},\text{OH}}$	3.67	0.337	0.00	0.00

Table S3. Group spin densities of UB3LYP/BS1 optimized geometries for the reaction pathway from $\text{Re}_{\text{Cl},\text{OMe}}$ as obtained in Gaussian-09.

	ρ_{Fe}	ρ_{ligand}	ρ_{OMe}	ρ_{SubCl}
${}^5\text{Re}_{\text{Cl},\text{OMe}}$	3.94	0.60	0.42	-0.96
${}^5\text{TS}_{\text{Cl},\text{OMe}}$	3.79	0.28	0.20	-0.27
${}^5\text{Pr}_{\text{Cl},\text{OMe}}$	3.67	0.33	0.00	0.00

Table S4. Group spin densities of UB3LYP/BS1 optimized geometries of ${}^6[\text{Fe}(\text{OH})(\text{N3PyO}^{2\text{Ph}})]^+$ and ${}^6[\text{Fe}(\text{OMe})(\text{N3PyO}^{2\text{Ph}})]^+$ isolated complexes as obtained in Gaussian-09.

	ρ_{Fe}	ρ_{ligand}	$\rho_{\text{OH}}/\rho_{\text{OMe}}$	ρ_{Total}
${}^6[\text{Fe}(\text{OH})(\text{N3PyO}^{2\text{Ph}})]^+$	3.99	0.54	0.46	5.00
${}^6[\text{Fe}(\text{OCH}_3)(\text{N3PyO}^{2\text{Ph}})]^+$	3.94	0.43	0.62	5.00

Table S5. Selected bond lengths of UB3LYP/BS1 optimized geometries of ${}^6[\text{Fe}(\text{OH})(\text{N3PyO}^{2\text{Ph}})]^+$ and ${}^6[\text{Fe}(\text{OMe})(\text{N3PyO}^{2\text{Ph}})]^+$ and associated transition states as obtained in Gaussian-09.

Bond/Structure:	(FeOMe) (Å)	(FeOH) (Å)	T _{ScI,OMe} (Å)	T _{ScI,OH} (Å)
Fe1-N1	2.445	2.378	3.759	3.551
Fe1-N2	2.290	2.282	2.293	2.297
Fe1-N3	2.283	2.303	2.335	2.289
Fe1-N4	2.181	2.165	2.207	2.179
Fe1-O1	1.933	1.921	1.967	1.936
Fe1-O2	1.790	1.815	2.004	1.962

Table S6. Absolute energies, zero-point energies and free energies (in au) of optimized geometries for the reaction of ${}^6[\text{Fe(OH)(N3PyO}^{2\text{Ph}}])^+$ with radical substrate (4-Cl-C₆H₄)₃C• as obtained in Gaussian-09.

	E [au]	ZPE [au]	G [au]	E _{solv} [au]
	B3LYP/BS1	B3LYP/BS1	B3LYP/BS1	B3LYP/BS2
${}^6[\text{Fe(OH)(N3PyO}^{2\text{Ph}}])^+$	-1882.278538	0.586526	-1881.759489	-1883.185227
${}^2(p\text{-Cl-C}_6\text{H}_4)_3\text{C}\bullet$	-2111.594199	0.251930	-2111.391251	-2112.067235
⁵Re_{Cl}	-3993.885858	0.840252	-3993.147419	-3995.254633
⁵TS_{Cl}	-3993.862927	0.840385	-3993.118221	-3995.227326
⁵Pr_{Cl}	-3993.901665	0.843577	-3993.156054	-3995.271148

Table S7. Relative energies, zero-point energies and free energies (in kcal mol⁻¹) of optimized geometries for the reaction of ${}^6[\text{Fe(OH)(N3PyO}^{2\text{Ph}}])^+$ with radical substrate (4-Cl-C₆H₄)₃C• as obtained in Gaussian-09.

	ΔE	ΔE+ZPE	ΔG	ΔE	ΔE+ZPE	ΔG
	BS1	BS1	BS1	BS2	BS2	BS2
⁵Re_{Cl}	-8.23	-7.11	2.08	-1.36	-0.24	8.96
⁵TS_{Cl}	6.16	7.37	20.41	15.77	16.98	30.02
⁵Pr_{Cl}	-18.15	-14.94	-3.33	-11.73	-8.51	3.09

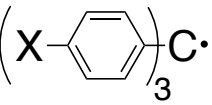
Table S8. Absolute energies, zero-point energies and free energies (in au) of optimized geometries for the reaction of $^6[\text{Fe}(\text{OMe})(\text{N3PyO}^{2\text{Ph}})]^+$ with radical substrate (4-Cl-C₆H₄)₃C• as obtained in Gaussian-09.

	E [au]	ZPE [au]	G [au]	E _{solv} [au]
	B3LYP/BS1	B3LYP/BS1	B3LYP/BS1	B3LYP/BS2
$^6[\text{Fe}(\text{OCH}_3)(\text{N3PyO}^{2\text{Ph}})]^+$	-1921.573786	0.616778	-1921.027713	-1922.489349
$^5\text{Re}_{\text{Cl},\text{OMe}}$	-4033.175592	0.868985	-4032.413975	-4034.562716
$^5\text{TS}_{\text{Cl},\text{OMe}}$	-4033.147358	0.869589	-4032.375258	-4034.529395
$^5\text{Pr}_{\text{Cl},\text{OMe}}$	-4033.191224	0.872016	-4032.421669	-4034.577266

Table S9. Relative energies, zero-point energies and free energies (in kcal mol⁻¹) of optimized geometries for the reaction of $^6[\text{Fe}(\text{OMe})(\text{N3PyO}^{2\text{Ph}})]^+$ with radical substrate (4-Cl-C₆H₄)₃C• as obtained in Gaussian-09.

	ΔE	$\Delta E+\text{ZPE}$	ΔG	ΔE	$\Delta E+\text{ZPE}$	ΔG
	BS1	BS1	BS1	BS2	BS2	BS2
$^5\text{Re}_{\text{Cl},\text{OMe}}$	-4.77	-4.60	3.13	-4.97	-3.67	4.06
$^5\text{TS}_{\text{Cl},\text{OMe}}$	12.94	13.50	27.43	17.06	17.61	31.54
$^5\text{Pr}_{\text{Cl},\text{OMe}}$	-14.58	-12.51	-1.70	-11.49	-10.90	-0.09

Table S10. Hammett parameters, rate constants, and redox potentials for the reaction of **1** with *para*-substituted radicals used during this study.

	$3\sigma^+_{para}^{11}$	k (M ⁻¹ s ⁻¹)	$E_{1/2}$, (V vs Fe ^{+/-}) ^a
-OMe	-2.33	25.5(2)	-0.58
-tBu	-0.77	13.4(1)	-0.25
-Ph	-0.54	6.8(8)	-0.19
-CN	1.98	2.5(3)	0.07

^a For the reaction: Ar₃C⁺ + e⁻ → Ar₃C• in CH₃CN at 25 °C.¹²

Derivation of Marcus Plot Analysis^{1,13}

For a given redox reaction:



The rate constant k_{ab} can be stated in terms of the free energy (ΔG^*_{ab}) of this reaction:

$$k_{ab} = Z_{ab} e^{-\frac{\Delta G^*_{ab}}{RT}} \quad (2)$$

$$\ln k_{ab} = -\frac{\Delta G^*_{ab}}{RT} + \ln Z_{ab} \quad (3)$$

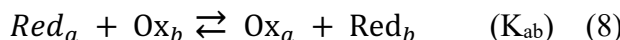
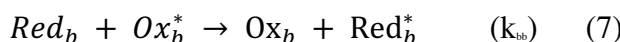
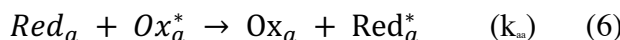
Z_{ab} is the frequency of collisions between a and b when in solution. ΔG^*_{ab} contains the sum of a series of 3 terms: a) the electrostatic work required to draw two ions together (w_{elec}), b) required energy to alter the solvent structure (ΔG^*_{solv}), and c) the necessary energy for the distortion of a metal-ligand bond-length (ΔG^*_{lig}):

$$\Delta G^*_{ab} = w_{elec} + \Delta G^*_{solv} + \Delta G^*_{lig} \quad (4)$$

When a reaction involves a molecule that is neutral, and an ion, w_{elec} is 0. Terms concerning ligand and solvent energy have been quantified by Marcus,¹⁴ and the derivation of such brought about the Marcus cross-relation:

$$k_{ab} = (k_{aa} k_{bb} K_{ab} f)^{1/2} \quad (5)$$

Elements k_{aa} and k_{bb} represent rate constants for exchange of electrons between oxidized and reduced states of an element (“self-exchange”), and K_{ab} is the defined equilibrium constant for the redox reaction between a and b. The element f is a function of the three terms k_{aa} , k_{bb} , and K_{ab} .



$$\ln f = \frac{0.25 (\ln K_{ab})^2}{\ln \frac{k_{aa} k_{bb}}{Z^2}} \quad (9)$$

With these definitions, equation 5 can then be re-written in the following:

$$\ln k_{ab} = 0.5 \ln K_{ab} + 0.5 [\ln k_{aa} + \ln k_{bb} + \ln f] \quad (10)$$

The Nernst equation can then be used to relate equilibrium constants K_{ab} to the standard redox potential E:

$$\Delta G^\circ = -nRt \ln K = -nFE^\circ \quad (11)$$

$$\ln K = \frac{F}{RT} (E_{red}^\circ - E_{ox}^\circ) \quad (12)$$

When substituting equations 9 and 12 into equation 10, while holding E_{red}° constant,

$$\begin{aligned} \frac{RT}{F} \ln k &= -0.5 E_{\text{ox}}^{\circ} + \\ [0.5 E_{\text{red}}^{\circ} + 0.5 \frac{RT}{F} \ln k_{aa} + 0.5 \frac{RT}{F} \ln k_{bb} + 0.5 \frac{RT}{F} (\frac{0.25 (\ln K_{ab})^2}{\ln \frac{k_{aa} k_{bb}}{z^2}})] & (13) \end{aligned}$$

The term E_{ox}° refers to the redox potential for the substrate undergoing oxidation. At the equilibrium conditions, $\Delta G^{\circ} \approx 0$, and $K_{ab} \approx 1$, the final term in equation 13 is cancelled. Because of that, when under limiting conditions, a simple linear free energy relationship is revealed by the Marcus theory, with a slope of $(RT/F) \ln k$ vs. E° of approximately -0.5 for a reaction having an ET rate-determining step. This slope of -0.5 is expected when ΔG° is small, otherwise large values of ΔG° bring about a $\ln(f)$ term that would no longer be ~0. For strongly endergonic reactions, the slope seen in a Marcus plot would approach -1.

VI. Cartesian coordinates.

⁶[Fe(OH)(N3PyO^{2Ph})]⁺:

26	-2.779077000	-0.194090000	0.075916000
6	-4.949669000	-2.055930000	3.897068000
1	-5.919476000	-2.478832000	3.653605000
6	-4.165662000	-2.650383000	4.889035000
1	-4.535091000	-3.522884000	5.417068000
6	-2.907726000	-2.119697000	5.199709000
1	-2.302564000	-2.574463000	5.976837000
6	-2.437662000	-0.995198000	4.509477000
1	-1.471435000	-0.569016000	4.759187000
6	-3.212860000	-0.402286000	3.506511000
1	-2.839884000	0.466802000	2.976129000
6	-4.477577000	-0.932899000	3.188567000
6	-5.356372000	-0.300192000	2.175116000
6	-6.706540000	-0.044196000	2.497297000
1	-7.063777000	-0.298369000	3.486943000
6	-7.549549000	0.561847000	1.571670000
1	-8.581134000	0.777340000	1.826334000
6	-7.043928000	0.900270000	0.310867000
1	-7.670943000	1.373091000	-0.436116000
6	-5.710779000	0.613924000	0.032252000
6	-5.121971000	0.819764000	-1.361849000
1	-5.797202000	1.462444000	-1.944888000
6	-5.050611000	-0.558782000	-2.006528000
6	-6.056740000	-1.010058000	-2.858305000
1	-6.848173000	-0.340411000	-3.175081000
6	-6.028839000	-2.345544000	-3.273875000
1	-6.797745000	-2.734220000	-3.932127000
6	-4.992308000	-3.164917000	-2.835188000
1	-4.931598000	-4.199715000	-3.148022000
6	-3.976270000	-2.648311000	-2.004861000
6	-2.855067000	-3.538681000	-1.611478000
6	-1.532210000	-3.242712000	-1.975425000
1	-1.318640000	-2.325479000	-2.510457000
6	-0.500245000	-4.133361000	-1.670140000
1	0.517303000	-3.903197000	-1.969355000
6	-0.777145000	-5.325552000	-0.990735000
1	0.025377000	-6.015797000	-0.752928000
6	-2.094817000	-5.630618000	-0.630293000
1	-2.316250000	-6.554462000	-0.106523000
6	-3.130706000	-4.748649000	-0.950260000
1	-4.151497000	-4.987957000	-0.668245000
6	-3.016737000	1.501902000	-2.541956000
1	-3.093986000	2.512666000	-2.961762000

1	-3.486121000	0.819124000	-3.258244000
6	-1.561915000	1.115132000	-2.390294000
6	-0.562360000	1.610227000	-3.235479000
1	-0.809612000	2.339713000	-3.998391000
6	0.751033000	1.163050000	-3.071274000
1	1.539705000	1.539732000	-3.712830000
6	1.039127000	0.232939000	-2.063458000
1	2.048171000	-0.127224000	-1.905006000
6	0.001504000	-0.218577000	-1.251134000
1	0.148621000	-0.933486000	-0.452106000
6	-3.794874000	2.756952000	-0.542944000
1	-4.406149000	2.620758000	0.353189000
1	-4.306934000	3.483419000	-1.192473000
6	-2.439069000	3.279293000	-0.148788000
6	-2.005453000	4.554498000	-0.534584000
1	-2.633192000	5.155720000	-1.187629000
6	-0.787598000	5.068783000	-0.075417000
1	-0.466320000	6.059084000	-0.378378000
6	0.006000000	4.299810000	0.787735000
1	0.947618000	4.695854000	1.153845000
6	-0.407627000	3.026595000	1.183422000
1	0.193377000	2.420249000	1.851668000
6	-1.629102000	2.503442000	0.718977000
7	-4.878482000	0.033823000	0.939662000
7	-4.023739000	-1.347570000	-1.590675000
7	-3.758031000	1.417834000	-1.246248000
7	-1.271449000	0.213939000	-1.422958000
8	-2.129059000	-1.694634000	0.863554000
1	-1.877047000	-1.951134000	1.766426000
8	-2.022055000	1.254792000	1.084074000

⁶[Fe(OCH₃)(N3PyO^{2Ph})]⁺:

26	-2.642980000	-0.528450000	-0.348958000
6	-5.277425000	-1.174314000	3.629331000
1	-6.192514000	-1.721376000	3.423504000
6	-4.644388000	-1.327542000	4.865054000
1	-5.074333000	-1.984771000	5.613443000
6	-3.461709000	-0.627828000	5.136850000
1	-2.977164000	-0.734282000	6.101832000
6	-2.910286000	0.210712000	4.161216000
1	-1.997820000	0.759679000	4.369103000
6	-3.529979000	0.356724000	2.915905000
1	-3.086947000	0.999351000	2.163785000
6	-4.724733000	-0.334058000	2.640410000
6	-5.471340000	-0.120421000	1.377528000
6	-6.859503000	0.130747000	1.441160000
1	-7.339469000	0.158328000	2.410808000
6	-7.585605000	0.386980000	0.283414000
1	-8.647160000	0.601050000	0.335963000
6	-6.921248000	0.384113000	-0.948347000
1	-7.450581000	0.588888000	-1.871665000
6	-5.556705000	0.111236000	-0.965036000
6	-4.795494000	-0.039464000	-2.279552000
1	-5.385611000	0.416655000	-3.087504000
6	-4.660329000	-1.533796000	-2.537696000
6	-5.554677000	-2.199638000	-3.374609000
1	-6.289844000	-1.643180000	-3.944690000
6	-5.488668000	-3.594428000	-3.446152000
1	-6.169043000	-4.147456000	-4.083919000
6	-4.525937000	-4.260211000	-2.692777000
1	-4.434023000	-5.337967000	-2.739868000
6	-3.622385000	-3.535099000	-1.888311000
6	-2.570324000	-4.284234000	-1.156039000
6	-1.209003000	-3.983459000	-1.328151000
1	-0.925322000	-3.147923000	-1.954569000
6	-0.228229000	-4.772239000	-0.720574000
1	0.820890000	-4.542225000	-0.876051000
6	-0.594398000	-5.867263000	0.072776000
1	0.168542000	-6.481152000	0.539622000
6	-1.948922000	-6.171671000	0.253366000
1	-2.240357000	-7.016616000	0.868033000
6	-2.930615000	-5.391549000	-0.364959000
1	-3.979584000	-5.632415000	-0.222411000
6	-2.561630000	0.363587000	-3.336637000
1	-2.605979000	1.213427000	-4.029244000
1	-2.929014000	-0.514412000	-3.878270000
6	-1.130765000	0.109572000	-2.919427000

6	-0.042510000	0.428196000	-3.739943000
1	-0.207208000	0.921472000	-4.691144000
6	1.249216000	0.117782000	-3.308836000
1	2.105027000	0.362034000	-3.927977000
6	1.426682000	-0.497806000	-2.062430000
1	2.415515000	-0.739772000	-1.692650000
6	0.303301000	-0.784276000	-1.290712000
1	0.369209000	-1.246559000	-0.314592000
6	-3.577977000	2.083015000	-1.857151000
1	-4.275491000	2.169789000	-1.020121000
1	-4.030394000	2.581286000	-2.728284000
6	-2.276695000	2.745580000	-1.496495000
6	-1.815897000	3.876467000	-2.184026000
1	-2.377397000	4.245738000	-3.038815000
6	-0.657293000	4.544331000	-1.773145000
1	-0.314241000	5.421372000	-2.310640000
6	0.047379000	4.077942000	-0.653771000
1	0.942067000	4.596010000	-0.323660000
6	-0.394626000	2.952285000	0.043450000
1	0.137325000	2.581929000	0.912605000
6	-1.557982000	2.273495000	-0.368314000
7	-4.839829000	-0.138446000	0.164898000
7	-3.705251000	-2.173615000	-1.812445000
7	-3.452559000	0.603447000	-2.158809000
7	-0.948788000	-0.494600000	-1.721310000
8	-2.110957000	-1.712571000	0.883492000
8	-1.977841000	1.167495000	0.297974000
6	-1.769868000	-2.514871000	2.008709000
1	-2.673970000	-2.766739000	2.575055000
1	-1.289914000	-3.440741000	1.672980000
1	-1.086326000	-1.968009000	2.669266000

$^5\text{TS}_{\text{Cl},\text{OH}}$:

26	-2.223588000	-0.006821000	0.451595000
6	-5.287667000	-0.959486000	4.046404000
1	-6.029561000	-1.696697000	3.755876000
6	-4.899597000	-0.865099000	5.384633000
1	-5.347454000	-1.522630000	6.122554000
6	-3.951676000	0.090079000	5.773130000
1	-3.676228000	0.190908000	6.817622000
6	-3.363758000	0.917816000	4.809612000
1	-2.620633000	1.651788000	5.101913000
6	-3.742318000	0.822638000	3.467273000
1	-3.280650000	1.473590000	2.733505000
6	-4.729451000	-0.103091000	3.073830000
6	-5.304074000	-0.060156000	1.707427000
6	-6.697785000	-0.173039000	1.555489000
1	-7.312085000	-0.351536000	2.428062000
6	-7.285391000	0.016625000	0.306784000
1	-8.360843000	-0.053499000	0.188308000
6	-6.470235000	0.341937000	-0.775360000
1	-6.890924000	0.530724000	-1.756419000
6	-5.088006000	0.415609000	-0.585117000
6	-4.207294000	0.730387000	-1.788933000
1	-4.708115000	1.527670000	-2.362573000
6	-4.142620000	-0.487402000	-2.710087000
6	-4.292573000	-0.349810000	-4.095090000
1	-4.426411000	0.627451000	-4.546184000
6	-4.293033000	-1.508326000	-4.881030000
1	-4.425031000	-1.441130000	-5.955463000
6	-4.153677000	-2.751356000	-4.267235000
1	-4.198274000	-3.655232000	-4.861109000
6	-4.004816000	-2.823025000	-2.865774000
6	-3.889049000	-4.113924000	-2.144090000
6	-4.197625000	-4.178478000	-0.771065000
1	-4.489700000	-3.269376000	-0.260463000
6	-4.145343000	-5.395569000	-0.087596000
1	-4.410210000	-5.433236000	0.964347000
6	-3.769891000	-6.568051000	-0.757874000
1	-3.742276000	-7.515800000	-0.229710000
6	-3.438911000	-6.510993000	-2.117215000
1	-3.137773000	-7.411497000	-2.642010000
6	-3.499522000	-5.296034000	-2.804425000
1	-3.226755000	-5.273295000	-3.854069000
6	-1.803949000	1.195542000	-2.369500000
1	-1.066269000	1.960958000	-2.101710000
1	-2.177600000	1.449737000	-3.371327000
6	-1.123423000	-0.150790000	-2.390645000

6	-0.475667000	-0.637420000	-3.530211000
1	-0.477092000	-0.051970000	-4.442685000
6	0.160654000	-1.880573000	-3.476684000
1	0.669093000	-2.272409000	-4.350655000
6	0.125533000	-2.612975000	-2.285103000
1	0.597747000	-3.584442000	-2.208696000
6	-0.535365000	-2.070558000	-1.184410000
1	-0.598739000	-2.580623000	-0.236857000
6	-3.063315000	2.686227000	-0.826403000
1	-3.805448000	2.615227000	-0.025506000
1	-3.499497000	3.294099000	-1.634630000
6	-1.809313000	3.347742000	-0.319533000
6	-1.390496000	4.580803000	-0.845634000
1	-1.953527000	5.024482000	-1.663409000
6	-0.279184000	5.252088000	-0.327425000
1	0.026114000	6.205757000	-0.743010000
6	0.426604000	4.681603000	0.740475000
1	1.285324000	5.197088000	1.159137000
6	0.030872000	3.454081000	1.275179000
1	0.560743000	3.013167000	2.112868000
6	-1.083501000	2.765829000	0.752836000
7	-4.505167000	0.194797000	0.621667000
7	-4.006286000	-1.690695000	-2.116157000
7	-2.872983000	1.264461000	-1.337862000
7	-1.138504000	-0.860125000	-1.234810000
8	-1.448321000	1.564568000	1.274216000
8	-1.823701000	-1.481185000	1.682248000
6	0.337163000	-2.255400000	2.991070000
6	-0.897650000	-1.311729000	6.429348000
6	-0.049916000	-0.242515000	6.728054000
1	-1.632786000	-1.643983000	7.150704000
6	-0.787470000	-1.935115000	5.191386000
1	-1.456499000	-2.752352000	4.951864000
6	0.172304000	-1.511733000	4.232075000
6	1.016661000	-0.422683000	4.581502000
6	0.906913000	0.209556000	5.816775000
1	1.569156000	1.025034000	6.079425000
1	1.796746000	-0.105189000	3.902673000
6	1.164645000	-1.742228000	1.902781000
6	1.132098000	-0.376461000	1.521379000
1	1.941548000	1.151526000	0.238863000
6	1.987983000	0.110409000	0.534474000
1	0.381828000	0.283980000	1.941524000
6	2.887300000	-0.764972000	-0.077786000
6	2.071000000	-2.604945000	1.235329000
6	2.939472000	-2.118915000	0.258436000

1	2.122828000	-3.650429000	1.514875000
1	3.651634000	-2.776540000	-0.224585000
6	0.559299000	-4.516974000	4.044582000
6	0.016900000	-3.705889000	3.020168000
6	-0.765985000	-4.318375000	2.019627000
6	-0.985526000	-5.696773000	2.027073000
6	-0.409701000	-6.470842000	3.034477000
6	0.359891000	-5.899577000	4.047259000
1	0.796347000	-6.518477000	4.821381000
1	1.167474000	-4.069842000	4.822982000
1	-1.605633000	-6.154614000	1.266534000
1	-1.266440000	-3.684243000	1.299158000
1	-2.401088000	-1.608845000	2.458789000
17	-0.192981000	0.571222000	8.339206000
17	4.006463000	-0.130949000	-1.359282000
17	-0.683339000	-8.266813000	3.035958000

⁵Re_{Cl,OH}:

26	-2.893970000	-0.307985000	-0.147365000
6	-5.745168000	-2.089605000	3.145613000
1	-6.578266000	-2.619973000	2.694636000
6	-5.188216000	-2.562704000	4.336373000
1	-5.595754000	-3.450842000	4.806770000
6	-4.104949000	-1.893501000	4.918184000
1	-3.676420000	-2.257788000	5.845507000
6	-3.579190000	-0.751641000	4.300061000
1	-2.750568000	-0.219394000	4.755564000
6	-4.124412000	-0.280606000	3.100778000
1	-3.706291000	0.599894000	2.626480000
6	-5.212300000	-0.950830000	2.509543000
6	-5.854948000	-0.446148000	1.272605000
6	-7.258736000	-0.321528000	1.224478000
1	-7.836924000	-0.592509000	2.098434000
6	-7.882317000	0.184007000	0.088065000
1	-8.960071000	0.297434000	0.057111000
6	-7.097210000	0.561317000	-1.006943000
1	-7.547433000	0.965681000	-1.906011000
6	-5.716250000	0.403541000	-0.923382000
6	-4.821684000	0.672953000	-2.126828000
1	-5.351678000	1.341730000	-2.820192000
6	-4.542910000	-0.648586000	-2.827284000
6	-5.000500000	-0.901039000	-4.118540000
1	-5.570651000	-0.151792000	-4.656036000
6	-4.701650000	-2.139598000	-4.699758000
1	-5.041862000	-2.374765000	-5.702026000
6	-3.978073000	-3.069847000	-3.962330000

1	-3.765060000	-4.050542000	-4.368040000
6	-3.548562000	-2.767693000	-2.650221000
6	-2.837223000	-3.805292000	-1.870492000
6	-3.215141000	-4.107530000	-0.550893000
1	-3.978011000	-3.515327000	-0.064161000
6	-2.606572000	-5.165434000	0.130501000
1	-2.909925000	-5.397474000	1.145561000
6	-1.604919000	-5.921420000	-0.489164000
1	-1.135135000	-6.740481000	0.045195000
6	-1.212985000	-5.620700000	-1.800259000
1	-0.434296000	-6.200946000	-2.284028000
6	-1.832351000	-4.576965000	-2.490546000
1	-1.525434000	-4.347510000	-3.506680000
6	-2.506500000	1.408958000	-2.769968000
1	-2.301980000	2.467610000	-2.960813000
1	-2.914717000	0.992254000	-3.698164000
6	-1.204030000	0.699730000	-2.456471000
6	-0.045169000	0.936815000	-3.205539000
1	-0.052911000	1.681617000	-3.993846000
6	1.113175000	0.209513000	-2.920103000
1	2.023618000	0.383055000	-3.482752000
6	1.089271000	-0.745713000	-1.895101000
1	1.970529000	-1.323403000	-1.647530000
6	-0.089980000	-0.930201000	-1.179037000
1	-0.188812000	-1.642077000	-0.370119000
6	-3.757440000	2.617283000	-0.992749000
1	-4.518797000	2.445701000	-0.227323000
1	-4.167687000	3.329753000	-1.724408000
6	-2.513458000	3.178587000	-0.359718000
6	-2.051874000	4.467241000	-0.657076000
1	-2.577521000	5.064653000	-1.397792000
6	-0.936666000	4.999759000	0.000601000
1	-0.592725000	6.000446000	-0.235845000
6	-0.274741000	4.234294000	0.970998000
1	0.587189000	4.643492000	1.487627000
6	-0.718361000	2.947297000	1.280753000
1	-0.219170000	2.342466000	2.029201000
6	-1.837058000	2.408325000	0.618644000
7	-5.102794000	-0.090076000	0.187287000
7	-3.826589000	-1.547760000	-2.102447000
7	-3.527129000	1.286600000	-1.679742000
7	-1.206853000	-0.212258000	-1.457820000
8	-2.265534000	1.151498000	0.909046000
8	-2.373130000	-1.718887000	0.910877000
6	3.406231000	-2.232108000	3.370409000
6	4.171654000	-0.876108000	6.834193000

6	5.559818000	-0.755602000	6.760867000
1	3.645403000	-0.586466000	7.735617000
6	3.474052000	-1.361415000	5.728931000
1	2.393922000	-1.435228000	5.779938000
6	4.142609000	-1.728866000	4.531466000
6	5.555234000	-1.586966000	4.504491000
6	6.261172000	-1.108431000	5.607466000
1	7.340397000	-1.021681000	5.576217000
17	6.475004000	-0.124793000	8.201219000
1	6.104014000	-1.882300000	3.617751000
6	3.884409000	-1.943248000	2.013684000
6	4.503190000	-0.706837000	1.693659000
1	5.388838000	0.536670000	0.167328000
6	4.934026000	-0.419078000	0.397905000
1	4.622109000	0.043642000	2.466472000
6	4.760522000	-1.377777000	-0.599713000
17	5.295226000	-0.998944000	-2.305950000
6	3.740756000	-2.890319000	0.966461000
6	4.179672000	-2.617806000	-0.330011000
1	3.305066000	-3.858904000	1.182669000
1	4.090153000	-3.363618000	-1.111202000
6	2.024760000	-3.908078000	4.646485000
6	2.182143000	-3.019038000	3.551677000
6	1.104212000	-2.922113000	2.633374000
6	-0.065497000	-3.666328000	2.790094000
6	-0.167634000	-4.528895000	3.881224000
17	-1.691937000	-5.514210000	4.098824000
6	0.862004000	-4.661474000	4.812257000
1	0.764858000	-5.348520000	5.644073000
1	2.834535000	-4.026158000	5.356876000
1	-0.876015000	-3.569893000	2.076776000
1	1.180550000	-2.234811000	1.798692000
1	-2.250103000	-1.671128000	1.877045000

⁵Pr_{Cl,OH:}

26	-2.962512000	-0.000870000	-0.288809000
6	-6.112739000	-0.244785000	3.512380000
1	-7.166373000	-0.315274000	3.260438000
6	-5.649774000	-0.810715000	4.702609000
1	-6.348368000	-1.299450000	5.373464000
6	-4.288708000	-0.745897000	5.028751000
1	-3.929442000	-1.171274000	5.960078000
6	-3.395629000	-0.113092000	4.155084000
1	-2.344060000	-0.042407000	4.412639000
6	-3.850432000	0.453701000	2.958475000
1	-3.151441000	0.977409000	2.312177000
6	-5.218096000	0.388322000	2.624140000
6	-5.740651000	0.985833000	1.372522000
6	-6.961256000	1.694440000	1.369067000
1	-7.485644000	1.847422000	2.303673000
6	-7.464128000	2.214256000	0.180473000
1	-8.394376000	2.771118000	0.175693000
6	-6.752123000	2.015191000	-1.009938000
1	-7.122031000	2.399122000	-1.953657000
6	-5.549530000	1.315670000	-0.953793000
6	-4.765739000	0.960275000	-2.219448000
1	-5.191004000	1.507176000	-3.072489000
6	-4.918683000	-0.544160000	-2.444983000
6	-5.679846000	-1.097535000	-3.472629000
1	-6.174956000	-0.460571000	-4.196427000
6	-5.788257000	-2.493438000	-3.543943000
1	-6.375312000	-2.955273000	-4.329785000
6	-5.153700000	-3.283412000	-2.586581000
1	-5.263037000	-4.360388000	-2.601075000
6	-4.397453000	-2.672592000	-1.567786000
6	-3.748443000	-3.451815000	-0.489773000
6	-3.721066000	-2.948147000	0.825848000
1	-4.202099000	-2.001076000	1.054302000
6	-3.156044000	-3.698858000	1.862933000
1	-3.170043000	-3.306622000	2.874517000
6	-2.607374000	-4.960762000	1.595157000
1	-2.192256000	-5.559259000	2.399757000
6	-2.621350000	-5.465193000	0.287195000
1	-2.194229000	-6.439656000	0.076777000
6	-3.190751000	-4.719439000	-0.747302000
1	-3.185242000	-5.114125000	-1.758120000
6	-2.436541000	0.831638000	-3.161251000
1	-2.118726000	1.701421000	-3.748511000
1	-3.027117000	0.195725000	-3.831387000
6	-1.211696000	0.052368000	-2.714441000

6	-0.060059000	0.018836000	-3.507970000
1	-0.016145000	0.599796000	-4.422617000
6	1.031023000	-0.752935000	-3.100244000
1	1.934223000	-0.782389000	-3.699493000
6	0.947039000	-1.469035000	-1.901632000
1	1.778077000	-2.060243000	-1.537917000
6	-0.225386000	-1.391709000	-1.149867000
1	-0.310941000	-1.905790000	-0.199850000
6	-3.036666000	2.704298000	-1.622458000
1	-3.760520000	2.943727000	-0.838514000
1	-3.239132000	3.362170000	-2.481072000
6	-1.637171000	2.948423000	-1.108951000
6	-0.827337000	3.928785000	-1.704456000
1	-1.190185000	4.448066000	-2.588592000
6	0.418534000	4.266003000	-1.168662000
1	1.027459000	5.029807000	-1.639134000
6	0.860074000	3.620629000	-0.005231000
1	1.816111000	3.889873000	0.433291000
6	0.075401000	2.636444000	0.599326000
1	0.399535000	2.136653000	1.505465000
6	-1.172866000	2.278682000	0.056242000
7	-5.046551000	0.819669000	0.210671000
7	-4.282300000	-1.318595000	-1.528694000
7	-3.307190000	1.271367000	-2.028841000
7	-1.288452000	-0.649164000	-1.552536000
8	-1.917888000	1.298499000	0.643165000
8	0.227430000	-2.826467000	1.742566000
6	1.310224000	-3.007770000	2.748047000
6	-0.895582000	-3.374171000	5.874723000
6	-0.643398000	-2.170967000	6.532315000
1	-1.588316000	-4.094091000	6.293469000
6	-0.224817000	-3.637604000	4.677833000
1	-0.395947000	-4.588585000	4.182949000
6	0.687685000	-2.714404000	4.128841000
6	0.925365000	-1.520735000	4.826585000
6	0.264766000	-1.243282000	6.031210000
1	0.461323000	-0.322483000	6.566720000
1	1.631309000	-0.796859000	4.439956000
6	2.384152000	-1.988077000	2.338161000
6	2.004821000	-0.779864000	1.726484000
1	2.661554000	1.089510000	0.867935000
6	2.962683000	0.168643000	1.352037000
1	0.958083000	-0.582246000	1.536041000
6	4.306804000	-0.092946000	1.606208000
6	3.747660000	-2.218346000	2.581443000
6	4.715134000	-1.272827000	2.221362000

1	4.072453000	-3.142947000	3.042606000
1	5.764910000	-1.459903000	2.410488000
6	2.443528000	-5.095681000	3.736569000
6	1.837389000	-4.450024000	2.645079000
6	1.770352000	-5.126440000	1.416132000
6	2.284528000	-6.419256000	1.276043000
6	2.876676000	-7.032621000	2.378182000
6	2.966985000	-6.387923000	3.609316000
1	3.431463000	-6.881040000	4.454375000
1	2.506660000	-4.597614000	4.697752000
1	2.230013000	-6.937559000	0.326331000
1	1.307747000	-4.635919000	0.568617000
1	-0.552865000	-3.359312000	2.002050000
17	-1.523405000	-1.812049000	8.088495000
17	5.559498000	1.138557000	1.117107000
17	3.544570000	-8.718019000	2.204321000

²(*p*-Cl-C₆H₄)₃C•:

6	0.630461000	-2.003122000	3.827277000
6	-0.423578000	0.960041000	5.954477000
6	0.621461000	1.866650000	5.726749000
1	-1.252742000	1.242745000	6.596586000
6	-0.414248000	-0.296646000	5.349562000
1	-1.236289000	-0.981543000	5.526208000
6	0.640534000	-0.690948000	4.479919000
6	1.692032000	0.242858000	4.272921000
6	1.682110000	1.494318000	4.889234000
1	2.505932000	2.181234000	4.718783000
1	2.528622000	-0.035109000	3.641751000
6	1.227345000	-2.203136000	2.503854000
6	1.286038000	-1.157595000	1.542309000
1	1.863647000	-0.546906000	-0.435867000
6	1.841879000	-1.363867000	0.279645000
1	0.861378000	-0.191096000	1.788124000
6	2.357352000	-2.618709000	-0.074693000
6	1.764055000	-3.464205000	2.122176000
6	2.314399000	-3.665240000	0.856391000
1	1.760073000	-4.277744000	2.838567000
1	2.725904000	-4.635808000	0.595453000
6	0.179032000	-3.368946000	5.897280000
6	-0.003377000	-3.147037000	4.510030000
6	-0.811893000	-4.069143000	3.799169000
6	-1.407015000	-5.156016000	4.443037000
6	-1.200142000	-5.366583000	5.812981000
6	-0.400108000	-4.469341000	6.533787000

1	-0.216067000	-4.635288000	7.591491000
1	0.799639000	-2.682755000	6.464322000
1	-2.032914000	-5.838912000	3.876469000
1	-0.984173000	-3.909069000	2.739924000
17	-1.942320000	-6.752849000	6.625594000
17	0.601671000	3.464170000	6.488614000
17	3.054809000	-2.878239000	-1.680650000

⁵TS_{Cl,OMe}:

26	-2.296249000	-0.171817000	0.663087000
6	-5.723347000	-0.868047000	4.018946000
1	-6.430367000	-1.629209000	3.704693000
6	-5.486597000	-0.675522000	5.381380000
1	-6.018308000	-1.278318000	6.110499000
6	-4.581340000	0.307169000	5.803657000
1	-4.422846000	0.484569000	6.862710000
6	-3.884549000	1.061542000	4.852963000
1	-3.173482000	1.816294000	5.171070000
6	-4.110853000	0.865852000	3.487241000
1	-3.560107000	1.455954000	2.764986000
6	-5.054922000	-0.084964000	3.053384000
6	-5.471934000	-0.137486000	1.630902000
6	-6.830748000	-0.331887000	1.327605000
1	-7.531455000	-0.522221000	2.129536000
6	-7.283301000	-0.200061000	0.016185000
1	-8.332448000	-0.338761000	-0.220051000
6	-6.375322000	0.169917000	-0.972313000
1	-6.697301000	0.334170000	-1.994204000
6	-5.027811000	0.328241000	-0.633056000
6	-4.060821000	0.773445000	-1.726774000
1	-4.528119000	1.645025000	-2.217151000
6	-3.949225000	-0.296747000	-2.811852000
6	-3.933600000	0.063292000	-4.165893000
1	-3.980617000	1.105269000	-4.463434000
6	-3.884005000	-0.952758000	-5.126824000
1	-3.890910000	-0.708274000	-6.183531000
6	-3.855207000	-2.282968000	-4.712831000
1	-3.857950000	-3.080170000	-5.445413000
6	-3.874232000	-2.580892000	-3.334383000
6	-3.865052000	-3.974187000	-2.826195000
6	-4.386436000	-4.259140000	-1.549306000
1	-4.784390000	-3.443919000	-0.957397000
6	-4.404954000	-5.568750000	-1.064858000
1	-4.825790000	-5.774823000	-0.085843000
6	-3.895542000	-6.616795000	-1.842520000

1	-3.916380000	-7.635139000	-1.468335000
6	-3.364625000	-6.343824000	-3.108682000
1	-2.963124000	-7.148712000	-3.715610000
6	-3.350274000	-5.034442000	-3.597182000
1	-2.917755000	-4.840296000	-4.573130000
6	-1.597552000	1.204079000	-2.053205000
1	-0.853739000	1.895723000	-1.640636000
1	-1.844022000	1.569503000	-3.060563000
6	-0.995712000	-0.176318000	-2.134213000
6	-0.265458000	-0.608839000	-3.246797000
1	-0.132166000	0.052873000	-4.095336000
6	0.275430000	-1.897356000	-3.251024000
1	0.844985000	-2.248312000	-4.104596000
6	0.058587000	-2.730624000	-2.147283000
1	0.443128000	-3.743276000	-2.126889000
6	-0.673152000	-2.234958000	-1.069603000
1	-0.891303000	-2.803611000	-0.177434000
6	-2.966450000	2.636043000	-0.551010000
1	-3.767576000	2.530042000	0.187269000
1	-3.333684000	3.302247000	-1.348718000
6	-1.746067000	3.244630000	0.086380000
6	-1.274172000	4.497195000	-0.338968000
1	-1.770618000	4.991468000	-1.170984000
6	-0.196858000	5.124267000	0.293430000
1	0.148950000	6.094151000	-0.046085000
6	0.419279000	4.486365000	1.378759000
1	1.249129000	4.966110000	1.888973000
6	-0.029732000	3.238687000	1.815340000
1	0.428509000	2.749002000	2.668395000
6	-1.110797000	2.590278000	1.177243000
7	-4.568970000	0.132821000	0.629627000
7	-3.931219000	-1.585488000	-2.411836000
7	-2.759902000	1.246909000	-1.132056000
7	-1.176290000	-0.979809000	-1.058852000
8	-1.521324000	1.371209000	1.605280000
8	-1.840012000	-1.812787000	1.718166000
6	0.424756000	-2.332930000	3.122627000
6	-1.445308000	-1.114609000	6.175569000
6	-0.591097000	-0.093378000	6.599848000
1	-2.349273000	-1.335086000	6.726380000
6	-1.130940000	-1.822136000	5.021191000
1	-1.811339000	-2.584379000	4.665634000
6	0.037418000	-1.524156000	4.275758000
6	0.871657000	-0.471943000	4.734012000
6	0.564495000	0.238613000	5.892571000
1	1.218346000	1.025038000	6.247964000

17	-1.000911000	0.824511000	8.105718000
1	1.789289000	-0.242671000	4.207705000
6	1.286383000	-1.749089000	2.099224000
6	1.102411000	-0.402215000	1.693843000
1	1.797178000	1.208298000	0.448847000
6	1.954789000	0.182604000	0.758924000
1	0.250856000	0.164825000	2.060130000
6	3.004633000	-0.571733000	0.231259000
17	4.116957000	0.188020000	-0.981198000
6	2.364166000	-2.483344000	1.538534000
6	3.225090000	-1.897544000	0.613162000
1	2.559579000	-3.496561000	1.868095000
1	4.062977000	-2.451744000	0.208908000
6	0.184173000	-4.477800000	4.408395000
6	0.232184000	-3.782582000	3.171736000
6	0.137142000	-4.548920000	1.981749000
6	-0.011313000	-5.932110000	2.018580000
6	-0.053845000	-6.576020000	3.258089000
17	-0.240459000	-8.373363000	3.310951000
6	0.048200000	-5.864134000	4.454333000
1	0.035200000	-6.385387000	5.403351000
1	0.301891000	-3.934550000	5.337085000
1	-0.103006000	-6.503650000	1.103501000
1	0.150551000	-4.041429000	1.028079000
6	-2.835548000	-2.796262000	2.044141000
1	-3.462330000	-3.043930000	1.172472000
1	-2.356644000	-3.736804000	2.360708000
1	-3.497418000	-2.461941000	2.854940000

VII. References.

- (1) Zaragoza, J. P. T.; Yosca, T. H.; Siegler, M. A.; Moënne-Locoz, P.; Green, M. T.; Goldberg, D. P., Direct Observation of Oxygen Rebound with an Iron-Hydroxide Complex. *J. Am. Chem. Soc.* **2017**, *139*, 13640-13643.
- (2) Jang, E. S.; McMullin, C. L.; Kass, M.; Meyer, K.; Cundari, T. R.; Warren, T. H., Copper(II) Anilides in sp³(3) C-H Amination. *J. Am. Chem. Soc.* **2014**, *136*, 10930-10940.
- (3) Dünnebacke, D.; Neumann, W. P.; Penenory, A.; Stewen, U., Stabile 4,4',4''-trisubstituierte Triphenylmethyl-Radikale. *Chem. Ber.* **1989**, *122*, 533-535.
- (4) Pangia, T. M.; Davies, C. G.; Prendergast, J. R.; Gordon, J. B.; Siegler, M. A.; Jameson, G. N. L.; Goldberg, D. P., Observation of Radical Rebound in a Mononuclear Nonheme Iron Model Complex. *J. Am. Chem. Soc.* **2018**, *140*, 4191-4194.
- (5) Gaussian 09, R. A.; Frisch, M. J.; Trucks, G. W.; Schlegel, H. B.; Scuseria, G. E.; Robb, M. A.; Cheeseman, J. R.; Scalmani, G.; Barone, V.; Mennucci, B.; Petersson, G. A.; Nakatsuji, H.; Caricato, M.; Li, X.; Hratchian, H. P.; Izmaylov, A. F.; Bloino, J.; Zheng, G.; Sonnenberg, J. L.; Hada, M.; Ehara, M.; Toyota, K.; Fukuda, R.; Hasegawa, J.; Ishida, M.; Nakajima, T.; Honda, Y.; Kitao, O.; Nakai, H.; Vreven, T.; Montgomery Jr., J. A.; Peralta, J. E.; Ogliaro, F.; Bearpark, M.; Heyd, J. J.; Brothers, E.; Kudin, K. N.; Staroverov, V. N.; Kobayashi, R.; Normand, J.; Raghavachari, K.; Rendell, A.; Burant, J. C.; Iyengar, S. S.; Tomasi, J.; Cossi, M.; Rega, N.; Milliam, J. M.; Klene, M.; Knox, J. E.; Cross, J. B.; Bakken, V.; Adamo, C.; Jaramillo, J.; Gomperts, R.; Stratmann, R. E.; Yazyev, O.; Austin, A. J.; Cammi, R.; Pomelli, C.; Ochterski, J. W.; Martin, R. L.; Morokuma, K.; Zakrzewski, V. G.; Voth, G. A.; Salvador, P.; Dannenberg, J. J.; Dapprich, S.; Daniels, A. D.; Farkas, Ö.; Foresman, J. B.; Ortiz, J. V.; Cioslowski, J.; Fox, D. J., Gaussian, Inc., C. T. Wallingford, 2009.
- (6) Becke, A. D., Density-functional thermochemistry. III. the role of exact exchange. *J. Chem. Phys.* **1993**, *98*, 5648-5652.
- (7) Lee, C.; Yang, W.; Parr, R. G., Development of the Colle-Salvetti correlation-energy formula into a functional of the electron density. *Phys. Rev. B* **1988**, *37*, 785-789.
- (8) Hay, P. J.; Wadt, W. R., *Ab initio* effective core potentials for molecular calculations. Potentials for the transition metal atoms Sc to Hg. *J. Chem. Phys.* **1985**, *82*, 270-283.
- (9) Ditchfield, R.; Hehre, W. J.; Pople, J. A., Self-Consistent Molecular-Orbital Methods. IX. An Extended Gaussian-Type Basis for Molecular-Orbital Studies of Organic Molecules. *J. Chem. Phys.* **1971**, *54*, 724-728.

- (10) Tomasi, J.; Mennucci, B.; Cammi, R., Quantum Mechanical Continuum Solvation Models. *Chem. Rev.* **2005**, *105*, 2999-3093.
- (11) Brown, H. C.; Okamoto, Y., Electrophilic Substituent Constants. *J. Am. Chem. Soc.* **1958**, *80*, 4979-4987.
- (12) Volz, H.; Lotsch, W., Polarographische Reduktion Von Triarylmethylkationen. *Tetrahedron Lett.* **1969**, 2275-2278.
- (13) Marcus, R. A.; Sutin, N., Electron transfers in chemistry and biology. *Biochim. Biophys. Acta., Rev. Bioenerg.* **1985**, *811*.
- (14) Marcus, R. A., On the Theory of Oxidation-Reduction Reactions Involving Electron Transfer. V. Comparison and Properties of Electrochemical and Chemical Rate Constants. *J. Chem. Phys.* **1963**, *67*, 853-857.
15. Cantú Reinhard, F. G.; Faponle, A. S.; de Visser, S. P. Substrate sulfoxidation by an iron(IV)-oxo complex: benchmarking computationally calculated barrier heights to experiment. *J. Phys. Chem. A* **2016**, *120*, 9805–9814.